



HAL
open science

Friction analysis during deformation of steels under hot-working conditions

Ivan Serebriakov, Eli Saúl Puchi-Cabrera, Laurent Dubar, Philippe Moreau,
Damien Méresse, José Gregorio La Barbera-Sosa

► **To cite this version:**

Ivan Serebriakov, Eli Saúl Puchi-Cabrera, Laurent Dubar, Philippe Moreau, Damien Méresse, et al.. Friction analysis during deformation of steels under hot-working conditions. Tribology International, 2021, 158, pp.106928. 10.1016/j.triboint.2021.106928 . hal-03445995

HAL Id: hal-03445995

<https://uphf.hal.science/hal-03445995>

Submitted on 7 Apr 2022

HAL is a multi-disciplinary open access archive for the deposit and dissemination of scientific research documents, whether they are published or not. The documents may come from teaching and research institutions in France or abroad, or from public or private research centers.

L'archive ouverte pluridisciplinaire **HAL**, est destinée au dépôt et à la diffusion de documents scientifiques de niveau recherche, publiés ou non, émanant des établissements d'enseignement et de recherche français ou étrangers, des laboratoires publics ou privés.

Friction analysis during deformation of steels under hot-working conditions

Ivan SEREBRIAKOV¹, Eli Saul PUCHI-CABRERA^{1,2,3}, Laurent DUBAR¹, Philippe MOREAU¹, Damien MERESSE¹, Jose Gregorio LA BARBERA-SOSA¹

¹LAMIH UMR CNRS 8201, Université Polytechnique Hauts-de-France, F-59313 Valenciennes cedex 9, France

⁽²⁾School of Metallurgical Engineering and Materials Science, Faculty of Engineering, Universidad Central de Venezuela, Postal address 47885, Los Chaguaramos, Caracas, 1040, Venezuela.

⁽³⁾Venezuelan National Academy for Engineering and Habitat, Palacio de las Academias, Postal Address 1723, Caracas 1010, Venezuela.

Abstract

An original multiscale friction analysis is developed to characterize the interfacial friction phenomena during the hot forging contact conditions in the manufacture of wheels for the railway industry. Hot upsetting sliding tests and roll-on-disc tests are performed to reproduce tribological conditions at meso and micro-scale.

Crushed and embedded oxides are found to be present on the sample's surfaces. Stick-slip phenomena occur in the roll-on-disc tests due to accumulation of the crushed oxides. This transform the interfacial contact conditions from a lubricant/oxide configuration to an oxide/oxide condition. Microanalysis measurements on the specimen's wear tracks clearly show that the lubricant layer is broken down and transferred from the tool to the specimen surface by means of the accumulated oxide particles.

Keywords

High temperature tribology; Hot forging process; Oxide scale behavior; Lubricant film; Stick-slip phenomenon

1. Introduction

In industrial hot-working processes employed in the manufacture of steel components, friction conditions at the tool/workpiece interface are severe due to the relatively high temperatures (850°C-1250°C) and loads involved in these operations. Under these processing conditions, the tool/workpiece interface usually involves the presence of an oxide layer and a

lubricant film. At these high temperatures, the oxide scale layer is mainly composed of an inner wüstite layer, besides the intermediate magnetite and outer hematite layers [1, 2]. The quantity of each oxide depends on the oxidation temperature [3]. Hematite can have a hardness of about 1000 HV at room temperature (RT) and promotes abrasive wear, whereas magnetite has a hardness of 500 HV at RT. On the other hand, wüstite is well known to have a lower hardness of 300 HV at RT and the highest lubricity among these oxides [4].

Basically, due to the elevated temperatures of the workpiece, lubricants for hot forming can only be applied to the tools. Thus, an appropriate lubricant should reduce friction and wear and be environmentally friendly [5]. The mechanical properties of the oxide scale and lubricant employed are important factors, which determine the magnitude of the friction coefficient at the tool/workpiece interface during hot forming. Therefore, it is important to understand the oxide and lubricant behavior, as well as their interaction when the friction analysis of an industrial hot forming process is conducted.

As shown in different investigations, the deformation behavior of the oxide layer formed on the surface of the steel components depends on a number of parameters. These include deformation temperature, strain applied, as well as oxide scale characteristics (thickness and composition) and surface topography, among others. As an example, Utsunomiya et al. [6] studied the hot rolling process of a low carbon JIS SS400 steel grade and determined that the oxide scale showed limited plasticity during deformation below 850°C. However, it was observed that the oxide scale ductility increased with the increase in temperature and the decrease in the scale thickness (< 26 µm). Furthermore, it was determined that the oxide layer could have an important lubricating effect during hot rolling, by decreasing the friction coefficient from 0.2 to 0.12 in the oxidized conditions. A similar study was conducted by Cheng et al. [7] on a 430 ferritic stainless steel hot rolled in the temperature range of 1050°C-1090°C. This investigation allowed the observation that thick oxide layers of iron oxides and Cr spinel formed on the alloy surface tended to fracture and pulverize during deformation, whereas thin layers tended to be plastically deformed at rolling reductions below 46%. Additional investigations on the hot rolling behavior of a micro-alloyed low carbon steel at 900°C carried out by Yu et al. [1] corroborated the significant effect of thickness reduction of the oxide scale behaviour. These authors reported that oxide cracking and blistering could be observed even if the material undergoes low rolling thickness reductions of about 3%, whereas, at higher thickness reductions (> 28%) the oxides were observed to be descaled.

The lubrication effect of the oxide layer formed on the steel surface has also been analyzed experimentally under compression testing conditions. In this sense, Matsumoto et al.

[8] investigated the behavior of a chrome JIS SCr420 steel grade deformed in the temperature range of 800°C-1150°C, by means of hot ring compression tests. According to these authors, the oxide layer can act as a lubricant during the hot forging processes, giving rise to a decrease in the friction coefficient from 0.6 to 0.3 when the oxide layer thickness increases from 6 μm to 300 μm . However, it was also observed that the oxide layer fractured and fragmented during the tests. Behrens et al. [9] also employed compression tests for investigating the flow stress behavior of different iron oxides at different temperatures and strain rates. For this purpose, cylindrical samples were sintered by employing iron oxides powder materials with different oxygen contents and deformed under hot compression conditions. The flow stress behavior was formulated on the basis of the Hansel-Spittel constitutive law. The numerical simulation of such tests showed that the forming force of a specimen covered by an oxide layer is expected to be less than that computed when the oxide layer is not present. The authors attributed these results to the smaller flow stress of the oxide scale, as compared with that of the steel substrate.

The oxide and lubricant interaction during deformation constitutes another important subject, which has also been analyzed in several previous studies [1, 2, 9–11]. Concerning this topic, Tran et al. [10] reported that the presence of an oxide layer formed onto a 316 stainless steel could provide undesirable tool sticking behavior during high temperature deformation and that it could be inhibited by means of a crystalline sodium borate lubricant. Also, Yu et al. [1] investigated the interaction between the oxide scale and nanoparticles of a graphite lubricant during the hot rolling of a micro-alloyed low carbon steel. A lubrication mechanism advanced by the authors proposed that the propagation of cracks along the magnetite grain boundaries could create a repository to collect graphite nanoparticles during lubrication, which could give rise to a decrease in the wear rate of the material. Kong et al. [11], on the other hand, studied the interaction of the oxide scale with a polyphosphate lubricant during the hot rolling of an interstitial-free (IF) steel. These authors reported that under unlubricated conditions, a significant number of cracks could be found in the oxide scale after deformation. However, under lubricated conditions, the oxide scale became compact and smooth. Similar results reported by Bao et al. [12] indicate that during hot rolling of an ASTM 1045 steel at 1000°C the oxide layer becomes thinner and denser under lubricated contact conditions due to the addition of 0.3 wt% of nano-SiO₂ particles.

The interaction between oxide scale and lubricants, which could occur during metal forming processes has also been recently investigated by means of wear tests. As an example, Wang et al. [2] studied the lubrication mechanisms of sodium metasilicate by means of ball-on-disc tests, aimed at reproducing the hot rolling contact conditions of a low C steel grade. For

this purpose, the tests were conducted at temperatures ranging from 550°C to 920°C, at a sliding velocity of 0.094 m/s and a normal load of 10 N. A low carbon steel and a high speed tool steel were used as disc and ball materials, respectively. The authors reported that during the sliding tests, melting at the interface occurred mainly due to the interaction between the outer hematite layer of the oxide scale and the sodium metasilicate film. Accordingly, the involvement of Fe^{3+} into the silicate melt contributes to the friction reduction under high temperature and pressure conditions.

Most of the investigations described above have mainly addressed the problems concerning the deformation behavior of the oxides and the oxide-lubricant interaction under different hot forming processing conditions. However, the problems concerning the lubricant film breakdown mechanisms by its interaction with an oxide layer under such conditions have been addressed to a much lesser extent. The present work proposes a multiscale research strategy to analyze in detail the mechanisms occurring at the tool/billet interface during the hot forging of an ER7 steel grade. For this purpose, hot upsetting-sliding tests as well as roll-on-disc tests were carried out under conditions similar to those found during the industrial practice. The evolution of the oxide layer and of the lubricant deposit are studied thanks to the surface topography, the evolution of the friction conditions and to EDS analyses.

2 Multiscale research strategy

The current research is based on a multiscale analysis of the hot forging interfacial contact conditions that exist at the tool-billet interface. The analysis has been conducted in order to study in more detail the tribological behavior of an ER7 steel grade deformed under hot forging conditions. This takes into account the oxide layer deformation behavior and its interaction with a lubricant film. According to the multiscale strategy, the interfacial contact conditions are analyzed at macro (industrial hot forging process), meso (hot upsetting sliding test) and micro scale (roll-on-disc tests). The macro-scale parameters are used to reproduce the forging contact including the severe material deformation and the oxide layer crushing at the meso-scale. Finally, a thin interfacial layer between the oxide and lubricant is reproduced under the hot forging conditions that allows us the understanding of the hot forging lubrication mechanism at the micro-scale level.

Figure 1 illustrates the multiscale research strategy.

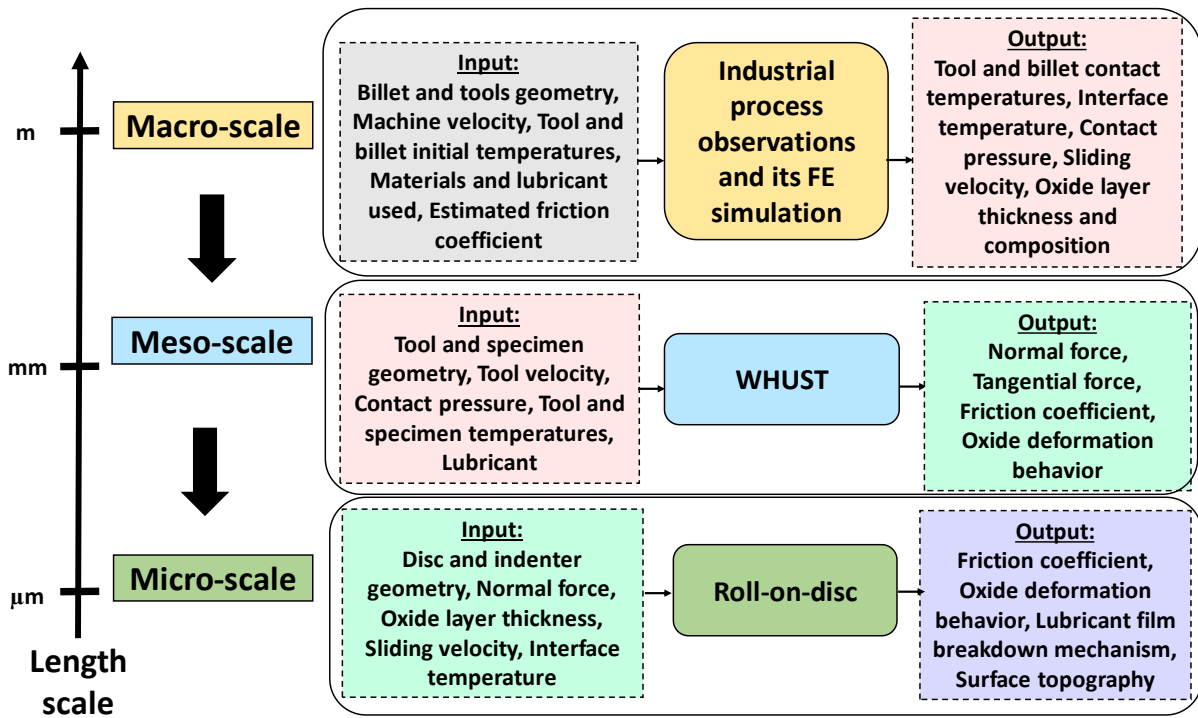


Figure 1. Multiscale research strategy

At the macro scale, the output parameters are determined by means of preliminary data obtained from the industrial process and Finite Element simulations based on the input parameters (billet and tools geometry, machine velocity, material and lubricant, etc.).

The obtained output parameters include: oxide layer thickness and composition, contacting temperatures, sliding velocities and contact pressures. The billet temperature at different locations is analyzed during the wheel forging by means of thermal camera measurements. Some oxide layer samples are collected at the industrial workshop. Also, the maximum press loads, as well as the processing and transporting times are gathered from the industrial process analysis. The other presented parameters (such as contact pressure, sliding velocity, etc.) were extracted from the FE model. These essential parameters influence the oxide layer tribological behavior and the lubricant film spallation under the hot deformation conditions. Based on the macro-scale output parameters (Figure 1), the meso-scale tests can be carried out in order to analyze the tribological conditions and oxide layer behavior under the hot forging contact conditions. To achieve it, the Warm and Hot Upsetting Sliding Test (WHUST) enables the application of severe conditions with plastic deformation and crushing of the specimen's asperities [13].

The device is illustrated on Figure 2 (b). The conditions determined in the vicinity of the contact zone at the macro scale are reproduced in this test in terms of plastic deformation and contact pressure. A schematic view of the tool/sample contact zone illustrates the principle of the test on Figure 2 (a). On the WHUST rig, the specimen is heated with an inductor close to the testing rig. It is then transported to the test area and fixed in the testing ring, as visible on Figure 2 (c). The tool is fixed on a moving part instrumented to obtain the normal and tangential load. The penetration of the tool is set according to the normal stress studied. This faithfully reflects the industrial process. The WHUST's results together with optical and SEM/EDS observations enable the analysis of the effect of the pair oxide-lubricant in the vicinity of the contact zone.

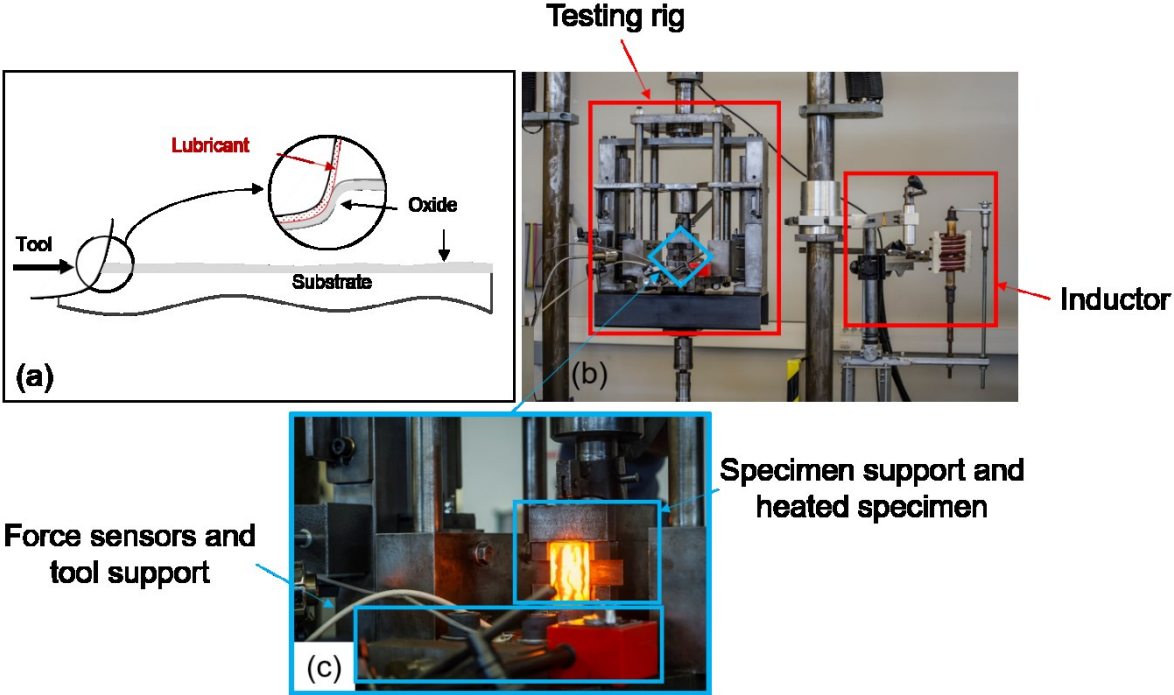


Figure 2. Meso-scale approach – (a) schematic view of the tool/sample contact zone during the WHUST, (b) picture of the WHUST rig, (c) sample in the testing area of the WHUST rig

The major input contact parameters of the WHUST are the tool and specimen geometry, sliding velocity, contact pressure, specimen and tool temperatures, etc (Figure 1).

The oxide deformation behavior and lubricant film break down mechanism are analyzed by applying the meso-scale output parameters (Figure 1) at the micro-scale by means of the original roll-on-disc test. In this configuration, a roll is in contact with a disc over its entire

generator and travels along the entire disc by rotating around its axis (Figure 3). This innovative test configuration makes it possible to know the response of the lubricant over a whole range of linear sliding velocities at a constant pressure and temperature. This test was designed to analyze the interfacial phenomena that occur at the billet/die interface due to the lubricating film, in particular the stick-slip mechanism and lubricant film break-down.

Also, these tests give the opportunity to study the sensitivity analysis of the tribological conditions to the input contact parameters such as the sliding velocity, contact pressure, lubricant type and temperature (Figure 1).

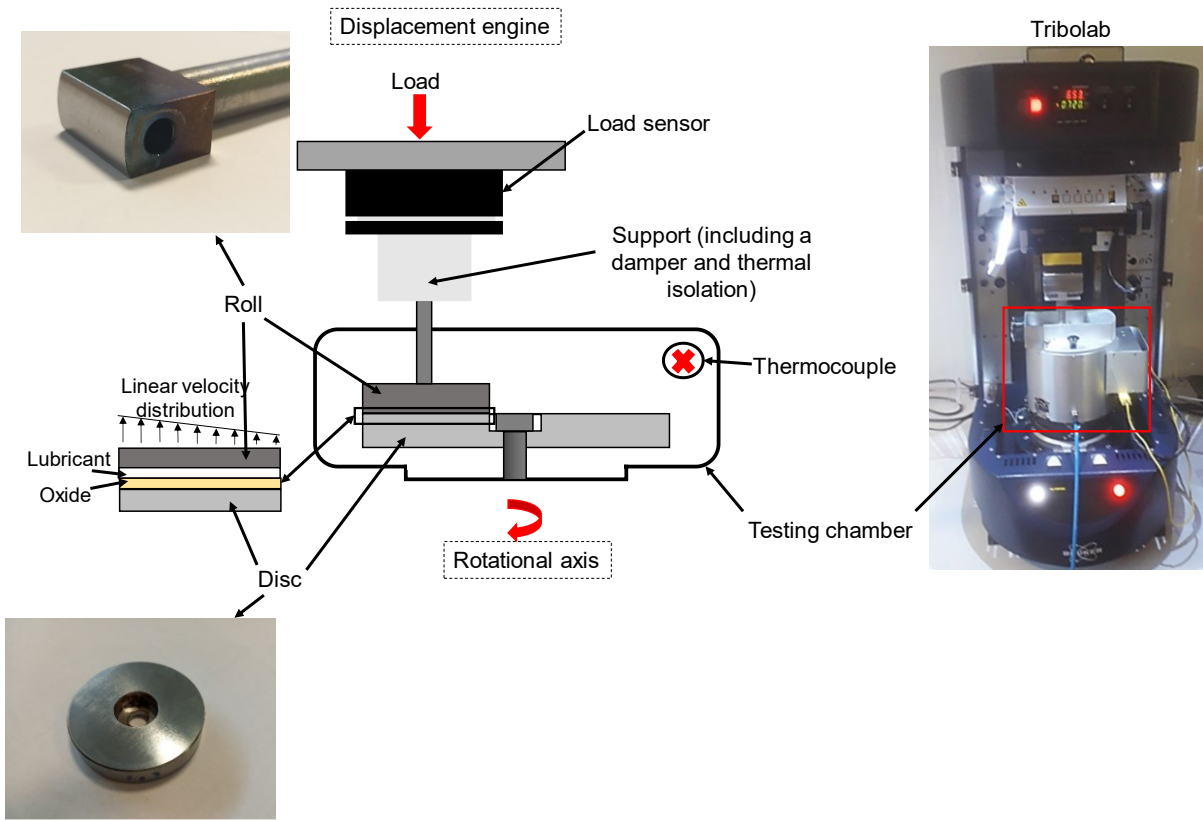


Figure 3. Micro-scale approach - schematic drawing of the roll-on-disc test and photographs of the tool, disc and Tribolab equipment

2.1 Macro-scale approach

The present research is related to the analysis of the friction conditions that take place in the first stage of the two-step hot forging process employed in the manufacture of wheels for the railway industry. The process is schematically described in Figure 4.

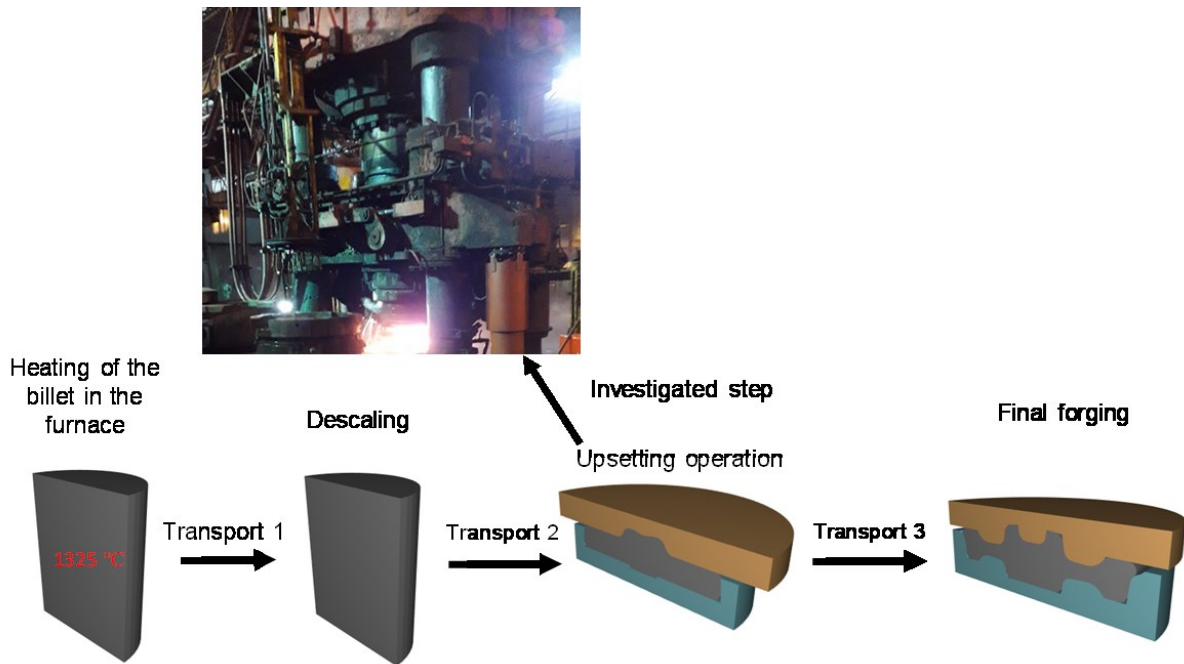


Figure 4. Schematic description of the wheel industrial hot forging process

An ER7 steel grade billet of 414 mm diameter and 525 mm height is preheated at 1325°C in a gas furnace during 4 hours. The chemical composition of the ER7 steel grade is given in Table 1. After heating, the billet is transported to be descaled. The forging tools, made of a C50 steel grade, are then sprayed with a 20% soap-water lubricant (ORAFOR WD – CONDAT) and the descaled billet is transported to them. The first forging operation (upsetting) is carried out on a hydraulic press with a maximum capacity of 3000 Tons. The upsetting height reduction for upsetting is of 70% with a press velocity of 40mm/s.

Table 1 Chemical composition of the ER7 steel grade according to the standard EN 13262 [14]

Maximum content in %wt.										
C	Si	Mn	P	S	Cr	Cu	Mo	Ni	V	Cr+, Mo+, Ni
0.52	0.40	0.80	0.02	0.015	0.30	0.30	0.08	0.30	0.06	0.5

Prior to descaling, the billet is covered with an oxide layer of approximately 4 mm in thickness. Subsequently, the descaled billet is subjected to re-oxidation. An oxide layer of about 65 µm is formed on its surface before the upsetting operation.

Thermal camera measurements were performed at the industrial workshop on the forging position by means of an infrared equipment (FLIR SC2500). The surface temperature

of the descaled billet before the first forging operation is observed to be of approximately 1200°C, whereas the temperature of the dies is found to be of about 200°C. Consequently, the tool/billet interface temperature can reach between 700°C and 800°C due to the heat generated by plastic deformation and friction.

2.2 Meso-scale approach

The friction analysis at meso-scale is conducted by means of the Warm Hot Upsetting Sliding Test. It can be used for reproducing the contact conditions of industrial forming processes and for the determination and identification of the constitutive friction laws [15].

In this testing rig, a tool comes into contact with a specimen and slides along its surface at the required contact sliding velocity. The cylindrical specimen is fixed in the support, whereas the tool is fixed perpendicular to the specimen; its position is precisely adjusted in order to localize the plastic deformation zone. To obtain the desired contact pressure, a relative penetration of the tool into the specimen is imposed before the start of the test. The tool and specimen geometries, as well as the penetration applied into the specimen are adjusted in order to obtain the desired contact pressure. The sliding velocity is controlled by means of a hydraulic cylinder. The tool and specimen are heated up by means of a heating cartridge and an inductor, respectively.

The contact parameters (pressure, sliding velocity and temperature) are determined during the macro-scale analysis, by means of FEM of the industrial forging process and subsequently reproduced. During the test, both the normal force (F_n) and shear force (F_t) are measured [13]. The friction coefficient along the track can be calculated as a function of F_n , F_t and the geometry of the contact [16, 17]. The sliding track and tool surfaces are used to analyze the material transfer and surface damage phenomena, which occur during the test.

On the other hand, the microscopic analysis of the contact surfaces allows the study of the oxide scale behavior during the contact.

After testing, the specimens are cooled down by compressed air and cut transversally in order to analyze the state of the remaining oxide scale and its microstructure. The wear tracks are analyzed by means of focus variation techniques (Alicona), scanning and optical microscopy.

2.3 Micro-scale approach

At the micro-scale level, the roll-on-disc tests are carried out by means of an UMT Tribolab mechanical tester (Bruker Corporation). Figure 3 illustrates a schematic drawing of

the roll-on-disc tests conducted in the present work. The essential parts of the testing rig are the cylindrical indenter (roll), disc and testing chamber. During the tests, the disk rotates, whereas the cylindrical pin is maintained fixed in the support. The temperature in the testing chamber is controlled by means of one thermocouple.

The aim of these tests is to investigate the lubricant film breakdown phenomena, as well as the oxide layer behavior and the oxide layer-lubricant interaction. The variables for the tests were the type of lubricant, sliding velocity, contact pressure and temperature. Due to the geometry of the roll (see Figure 3), each test is performed in a range of sliding velocities according to the rotating speed of the disc. The influence of the sliding velocity on the friction phenomenon is then analyzed in these range. The testing conditions are presented in Table 2 with the correspondence between the rotating speed and the sliding velocity ranges.

Table 2. Roll-on-disc testing conditions

Test condition No.	Temperature (°C)	Contact pressure (MPa)	Rotating speed (rpm)	Lubricant
1	700	200	21	20% soap-water mixture
2	800		(16 to 50 mm/s)	
3	700	100	21 (16 to 50 mm/s)	20% soap-water mixture
4		250		
5	700	200	4.8 (4 to 12 mm/s)	20% soap-water mixture
6			47.7 (40 to 125 mm/s)	
7	700	200	21 (16 to 50 mm/s)	Without lubricant

The basic testing conditions implies conducting the roll-on-disc tests at a temperature of 700°C, a mean pressure of 200 MPa, an operating speed of 21 rpm (16 to 50 mm/s) and the use of a 20% soap-water mixture as lubricant. These conditions are slightly modified by including an additional temperature of 800°C, operating speeds of 4.8 rpm (4 to 12 mm/s) and 47.7 rpm (40 to 125 mm/s), as well as testing without lubrication, which allows the analysis of the sensitivity to these parameters. At least two samples are tested for each condition.

The tests are performed employing a C50 grade steel cylindrical roll with a radius of 20 mm, against ER7 steel discs with diameter of 51 mm. Bars of 55 mm diameter and 300 mm

height are employed for machining the discs used in the roll-on-disc tests. Prior to the tests, the lubricant is deposited on the indenter for 10 s in a lubricant bath, in order to create a lubricant film similar to that found in the industrial forging practice.

The test parameters are chosen close to the industrial hot forging conditions in order to observe the behavior of the oxides under similar interfacial characteristics.

1. In the first step, the disc is heated up to 1000°C during 90 min in a heating chamber while the pin was kept at room temperature.
2. In the second step, when the temperature reached 1000°C, the disc is cooled down to room temperature at 5°C per minute in argon. Thus, an oxide layer of 65 µm is formed on the disc surface.
3. In the third step, the disc and pin are heated up together in argon to the prior computed interface temperature. The latter varies from 700°C to 800°C during the hot forging process.

During the preliminary testing stage, the disc and pin temperature are monitored by means of a K-type thermocouple welded on their surfaces. The duration of the wear test is of approximately 3 s for an operating speed of 21 rpm, corresponding to one full turn around the disc. Finally, the pin and disc are cooled down inside the heating chamber.

After testing, the wear track is analyzed by means of focus variation techniques (Alicona), as well as scanning and optical microscopy. In addition, the samples are also cut transversally in order to analyze the state of the remaining oxide scale and its microstructure. With the purpose of preserving the oxide scale, specimens are encapsulated with a phenolic resin before cutting them with an abrasive disc at a feed speed of 0.01 mm/s. After cutting, the exposed surface is prepared metallographically. The grinding step is carried out using abrasive discs (MD-Piano 220 and MD-Piano 500). The polishing step involves the use of diamond abrasive suspensions with particle sizes of 9, 3 and 1 µm.

3. Results

3.1 Macro-scale results: sliding velocity, contact pressure and temperature profile

The FEM simulations are also used to identify the essential contact parameters which characterize the forging process, such as sliding velocity, contact pressure, tool and billet temperature, as well as interface temperature. These thermomechanical simulations are conducted employing the code Forge NxT 3.0 (TRANSVALOR S.A.). A 2D axisymmetric model is used with a tetrahedral mesh for modeling the billet and dies. The elements for the dies are considered to be rigid. The initial mesh element size varies in the range from 5 to 10

mm. The elements are automatically re-meshed each time the element geometry requires it, according to an angular criterion. The initial number of elements is 146000. The forging equipment is a hydraulic press with a maximum capacity of 3000 Tons and a ram speed of 40 mm/s. For the modelling, the hydraulic press is chosen from the Forge NxT professional software database. The flow stress behavior of the ER7 steel at the forging temperature is computed by means of the Hansel-Spittel constitutive law [18] derived for the temperature range of 850°C - 1250°C, up to effective strains of 0.9 and effective strain rates in the range of 0.005 to 10 s⁻¹ (Equation 1) :

$$\sigma = 5500 e^{(-2.61 \cdot 10^{-3} T)} \dot{\epsilon}^{0.307} (\dot{\epsilon})^{-0.165} e^{\frac{-6.61 \cdot 10^{-4}}{\dot{\epsilon}}} (1 + \epsilon)^{-2.55 \cdot 10^{-3} T} e^{0.725 \epsilon} \epsilon^{3.41 \cdot 10^{-4} T} T^{-0.069} \quad \text{MPa} \quad (1)$$

The initial temperatures of the billet and the tools are 1325°C and 200°C respectively. The heat exchange coefficient with air is set at 8W/m²/°C and the heat transfer coefficient at the billet/tool interface is chosen at 3000 W/m²/°C

The maximum sliding velocity is deduced from the velocity map along the radial axis. This can be considered as the sliding velocity in the contact area as the tool is modelled by a rigid part and does not move in the x-y plane. The maximum sliding velocity is of approximately 40 mm/s (Figure 5 (a)) and the maximum contact pressure is about 200 MPa (Figure 5 (b)) on the upper side of the billet. The billet and tools temperature are in the range of approximately 1000°C-1100°C (Figure 5 (c)) and 390°C-470°C, respectively.

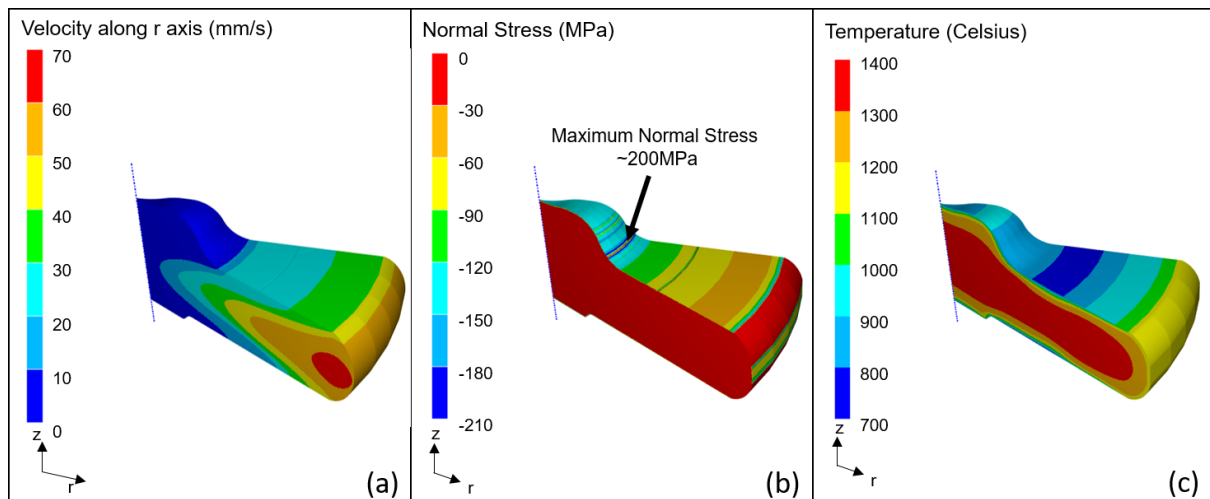


Figure 5. FEM simulation of the wheel forging: (a) sliding velocity field; (b) contact pressure field; (c) temperature field

Also, according to the FEM simulations, in the first forging step, the material undergoes an effective strain of about 3.5, at increasing strain rates from 0.005 to 1 s⁻¹.

3.2 Meso-scale results: friction tests and microstructural observations

Cylindrical samples of the ER7 steel grade of 30 mm diameter and 48 mm height were preheated by induction in air at a temperature of 1150°C during 5 min in order to grow a representative oxide scale layer of approximately 65 μm, prior to the WHUSTs. The specimen testing temperature is controlled by means of a pyrometer. The tests are conducted both with and without lubrication at a temperature of 1050°C, employing contact pressures in the range of 150-200 MPa and a sliding speed of 40 mm/s according to the macro-scale results. The maximum sliding distance achieved is around 45 mm.

The tools employed in the WHUSTs are made of C50 steel grade. These have a contact radius of 20 mm and are maintained at a temperature of 200°C. The initial penetration of the tool varies between approximately 300 and 400 μm, depending on the contact pressure required. All the experimental samples are machined from an actual billet employed in the industrial forging process. The billet is machined into a number of steel bars of 35 mm diameter and 150 mm height. Afterwards, these bars are employed for machining the samples for the WHUST.

Figures 6 through 8 show the results of some of these tests that were conducted at a temperature of 1050°C, a sliding velocity of 40 mm/s and a mean pressure of 200 MPa. Figures 6 (a) and (b) illustrate the evolution of the friction coefficient along the sliding track for the non-lubricated and lubricated conditions, respectively. The friction coefficient is calculated between 5 and 40 mm to avoid the edge effect on the piece. The mean contact pressure is generally not reached before 5mm due to the chamfer. The analysis of such curves indicates that the 20% soap-water lubricant has an important effect on the friction coefficient under the applied contact conditions. Under the non-lubricated conditions, the mean friction coefficient varies from 0.52 to 0.83 along the track (Figure 6 (a)), whereas, under the lubricated conditions it is observed that the mean friction coefficient varies from 0.2 to 0.76 (Figure 6 (b)).

Figure 6 (b) shows that full lubricant film exhaustion seems to be achieved at a sliding distance around 26 mm. From 5 mm to 26 mm, the coefficient of friction evolves almost linearly from 0.25 to 0.5, then increases rapidly, after an additional 5 mm displacement, to 0.7, before stabilization. From 5 mm to 26 mm, the upward trend could be associated with the lubricant film depletion. Subsequently, after 26 mm, a transformation of the contact conditions from the

oxide/lubricant to oxide/steel or even oxide/oxide contact, at the end of the sliding track, takes place.

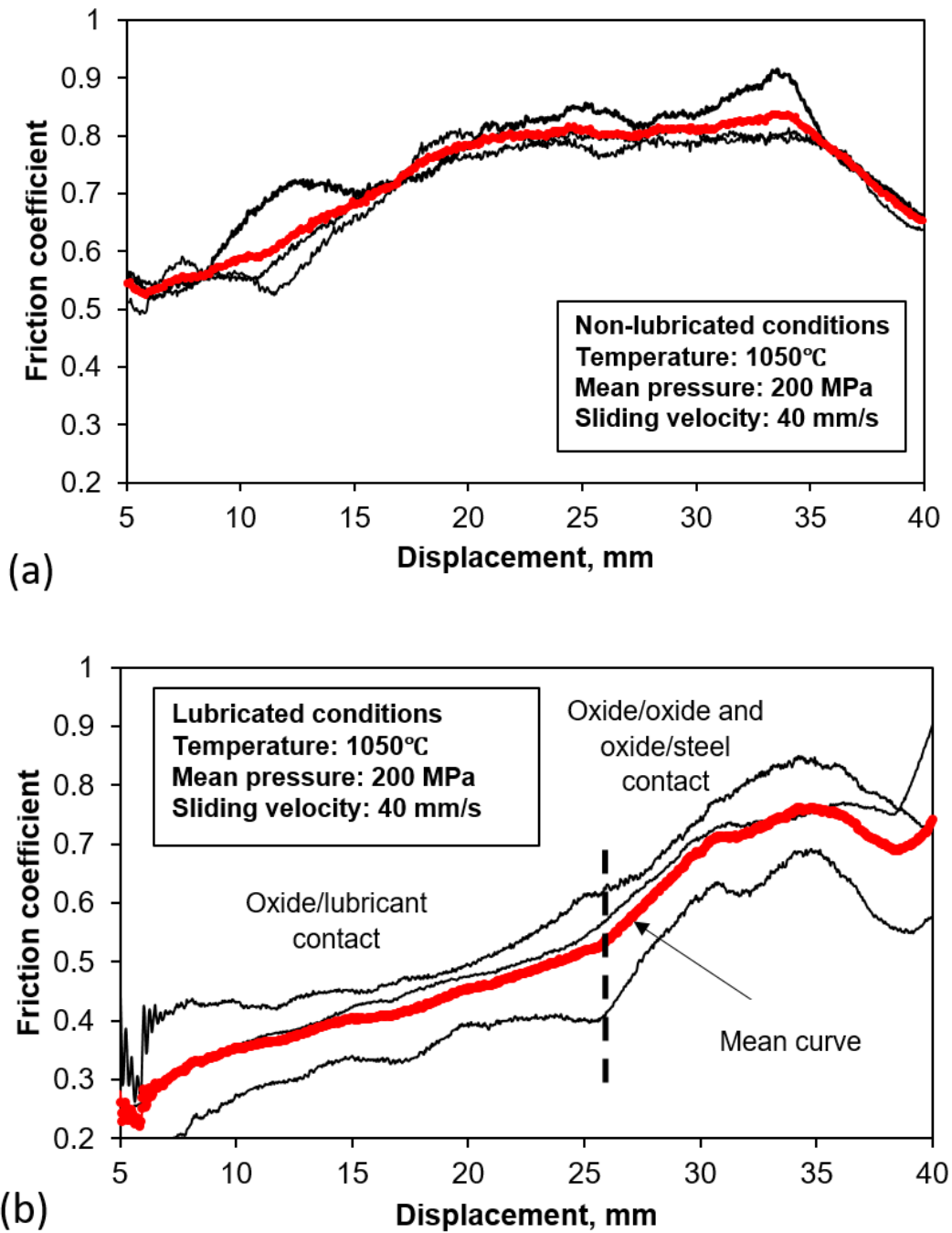


Figure 6. Friction coefficient evolution along the sliding track: (a) non-lubricated conditions; (b) lubricated conditions.

An optical observation of the sliding track for the test under lubricated conditions is presented in Figure 7 (a). As can be observed in Figure 7 (b), there are a significant number of cracks at the beginning of the track, whereas, less or even no cracks can be seen in the middle

and at the end of it (Figure 7 (c) and (d)). Thus, the specimens are cut transversely along the track and metallographically prepared to analyze the oxide scale deformation behavior on a cross-sectional plane.

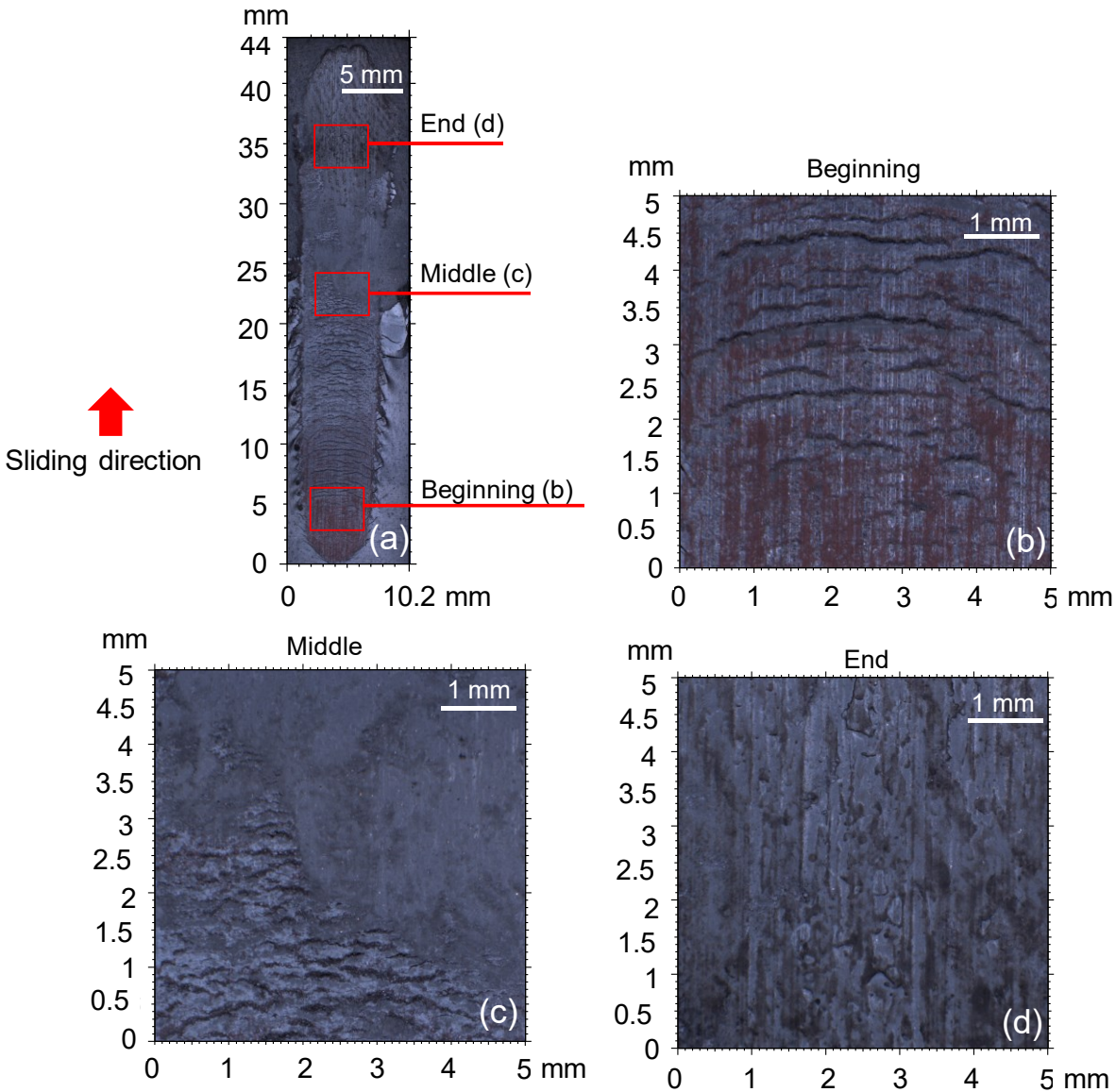


Figure 7. Sliding track of the WHUST sample under lubricated conditions: (a) sliding track global view; (b) beginning; (c) middle; (d) end of the sliding track

Figure 8 shows the SEM/EDS images of the oxide-steel interface cross-section. They allow providing more detailed information of the steel/oxide interface.

The iron and oxygen EDS maps allow the identification of different oxide layers present at the interface. Figure 8 (a) illustrates that three different layers of the oxide scale are present at the beginning of the track. The first one corresponds to the innermost compact embedded

layer located on top of the substrate. Above this, an intermediate crushed oxide layer can be observed and on top of the latter, an outermost secondary oxide layer formed after deformation. As shown in Figure 8 (b), only two layers can be observed in the middle of track, the innermost crushed layer and outermost oxide layer.

Similarly, in Figure 8 (c) a two layered structure can be observed including the innermost crushed layer and the outermost compact layer. Additionally, at this position, the oxides displaced by the tool during the deformation under the deformed steel layer can be seen. Under the contact conditions employed, the contacting oxides exhibit mainly a brittle deformation behavior. These deformed oxides can be responsible for the lubricant film breakdown mechanism. The micro-scale tests are designed to study the lubricant depletion mechanism and its interaction with the deformed oxides.

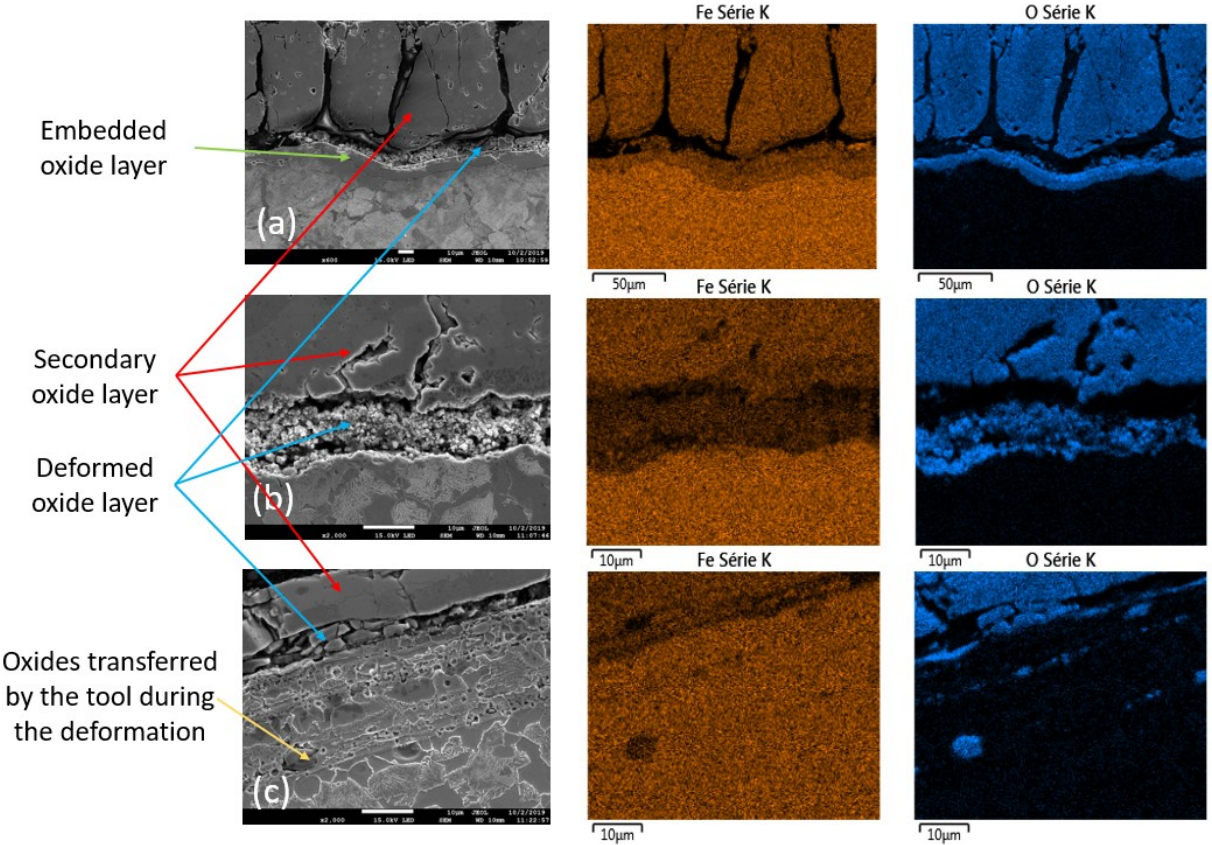


Figure 8. SEM/EDS cross-section analysis of the WHUST specimen deformed under lubricated conditions: (a) beginning; (b) middle; (c) end of the track.

3.3 Micro-scale results
3.3.1 Analysis of roll-on-disc tests

Figure 9 illustrates the friction coefficient and sliding velocity evolution curves along the sliding track for the lubricated conditions during a roll-on-disc test (test condition No. 1). The temperature is set to 700°C, the operating speed is 21 rpm and a mean pressure of 200 MPa is applied. Even if the test conditions were different, the similar evolution of the coefficient of friction as in the work of Zambrano et al [19] is found: a rise in speed and then a stabilized zone where the coefficient of friction varies significantly. The oscillation of the friction coefficient and operating speed are possibly due to a micro-scale stick-slip phenomenon. As can be seen along the sliding distance, a number of peaks on the friction coefficient curve are associated with a significant decrease in the sliding velocity, which highlights the occurrence of a jerky-type slip, typical of a stick-slip mechanism.

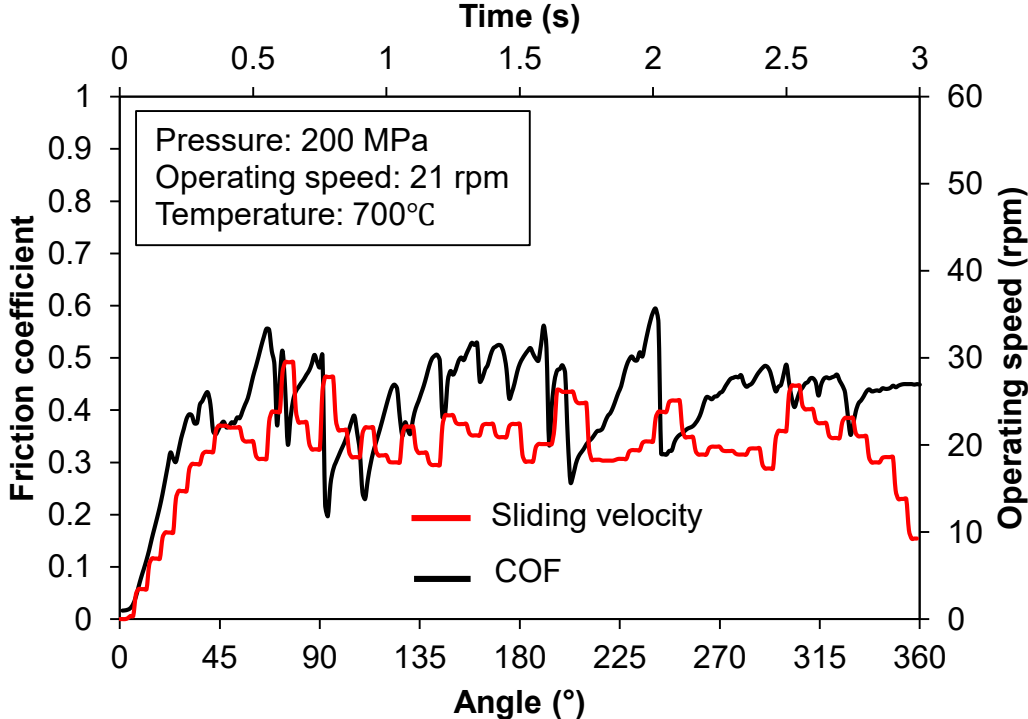


Figure 9. Friction coefficient and sliding velocity evolution during a lubricated roll-on-disc test (test condition No. 1)

The occurrence of the stick-slip phenomenon under hot deformation conditions at micro-scale could be associated with the accumulation of the crushed oxides at the tool/disc contact zone. The oxide layer can exhibit different types of behavior, such as that observed at the meso-scale (section 3.2). Thus, during the roll-on-disc tests, deformed and embedded oxides

were also found to be present on the specimen surface (Figure 10), similar to those previously observed in the WHUST samples after testing.

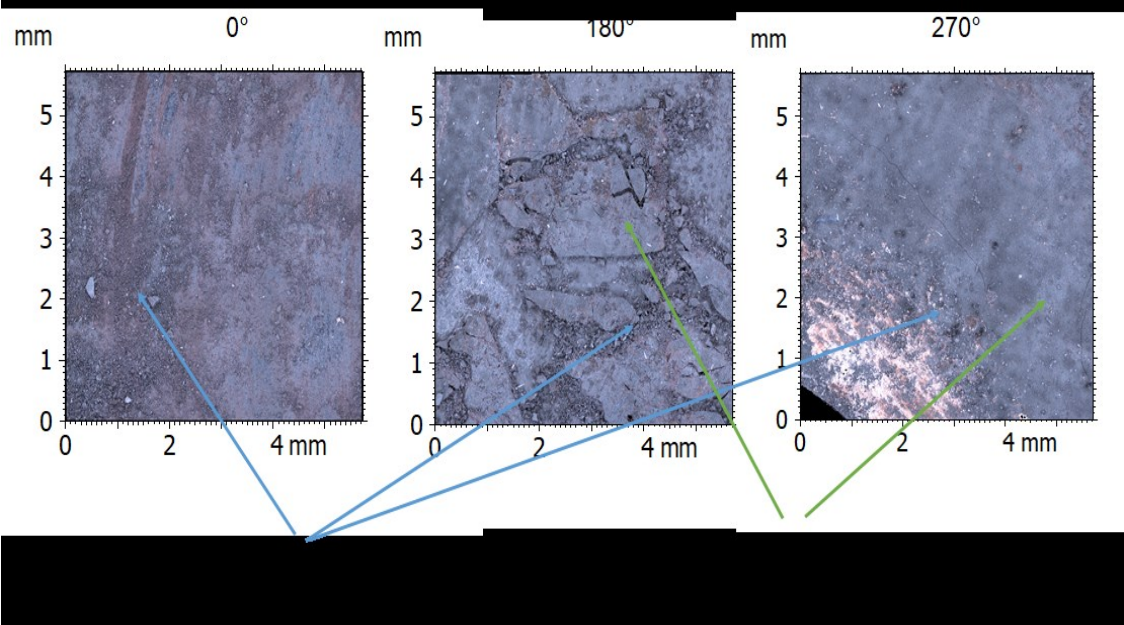


Figure 10. Different zones of the roll-on-disc sample after testing under lubricated conditions (Test condition n°1).

Figure 11 (a) shows the oxidized disc 3D surface topography of an undeformed disc, before the roll on disc test. On Figure 11(b) the surface topography of the disc shows important differences after a roll-on-disc test in the Condition n°1. The retained oxide surface topography image can be used to analyze the oxide accumulation and subsequent stick-slip phenomenon, as previously described in Figure 9.

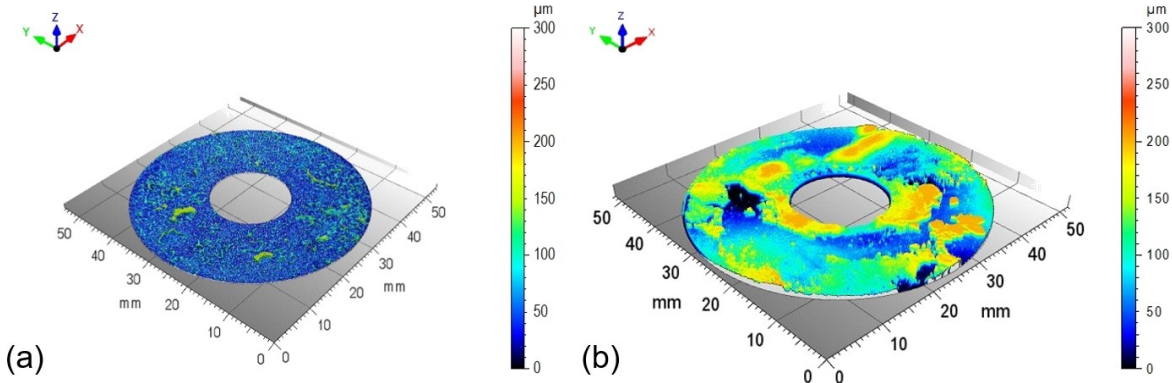


Figure 11. 3D surface topography of (a) the undeformed disc and (b) the tested specimen (Test Condition n°1).

The 3D topography of the first characteristic zone of the specimen is shown in Figure 12 (a). This zone is located at a counter clockwise rotation between 45° and 90° from the indenter initial position and corresponds to the depletion of the lubricant film effect on the indenter. Figure 12 (b) illustrates the change in the sliding velocity and friction coefficient along this particular track, located on the disc edge, in the area where the oxides have accumulated. Figure 12 (c) on the other hand, shows the corresponding change in the surface roughness profile at the edge (I), middle (II) and center (III) of the disc, respectively. As can be observed in Figure 12 (a), the blue zones correspond to the descaled specimen surfaces, whereas the green-yellow areas located at a sliding distance between approximately 10-15 mm represent an increase in the oxide height due to its displacement and accumulation. Figures 12 (b) and (c-I) clearly show that the friction coefficient peaks labeled as (1) and (3) correspond to the peaks on the roughness profile, whereas the friction coefficient valleys (2) and (4) correspond to the valleys on the roughness profile. The lack of correspondence in Figures 12 (c-II) and (c-III) can be explained by the small quantity of the accumulated oxides.

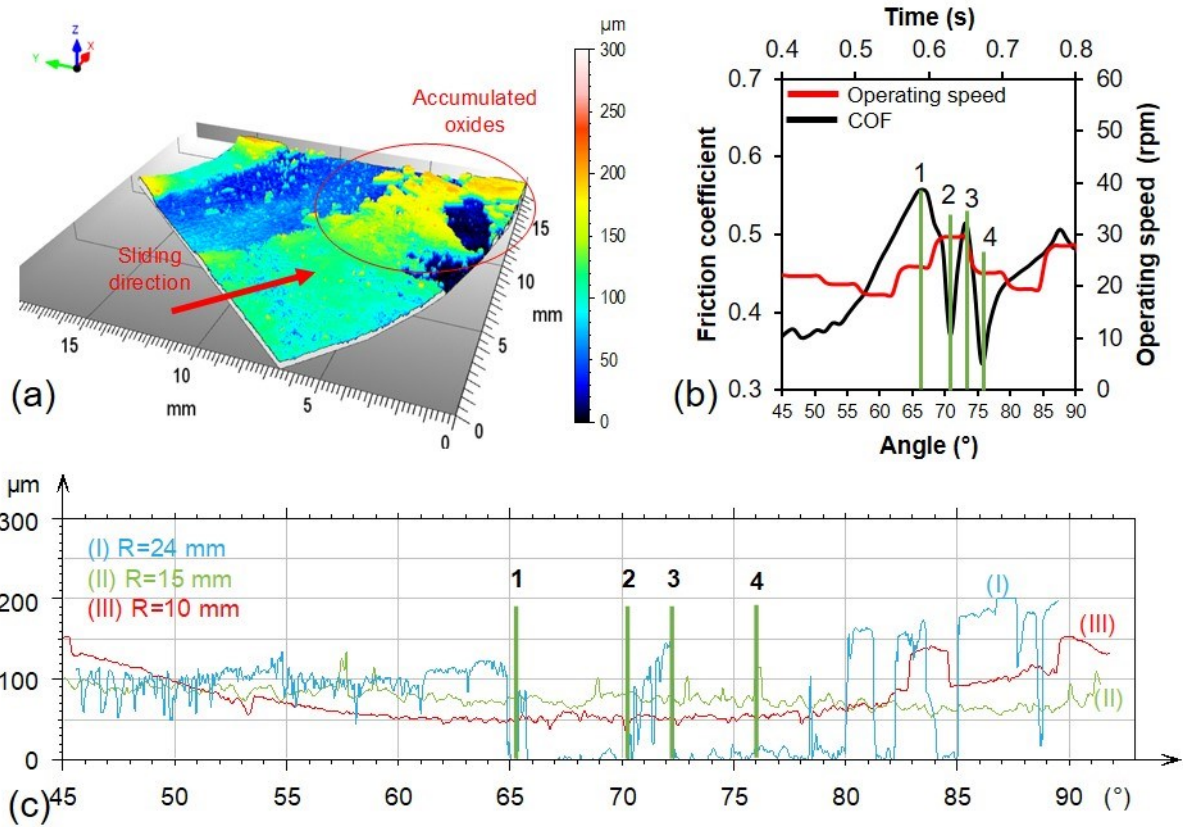


Figure 12. First characteristic zone on the disc surface for Test Condition n°1: (a) 3D surface topography; (b) COF and operating speed curves as a function of the indenter rotation; (c) surface roughness profiles at the edge (I), middle (II) and center (III)

Additionally, the surface roughness profile in the radial direction at an angle of 65° for the first characteristic zone on the disc surface is measured (Figure 13). The most of the accumulated oxides are located at the edge of the disc, which corresponds to the plateau between 18 and 24 mm at the surface roughness profile.

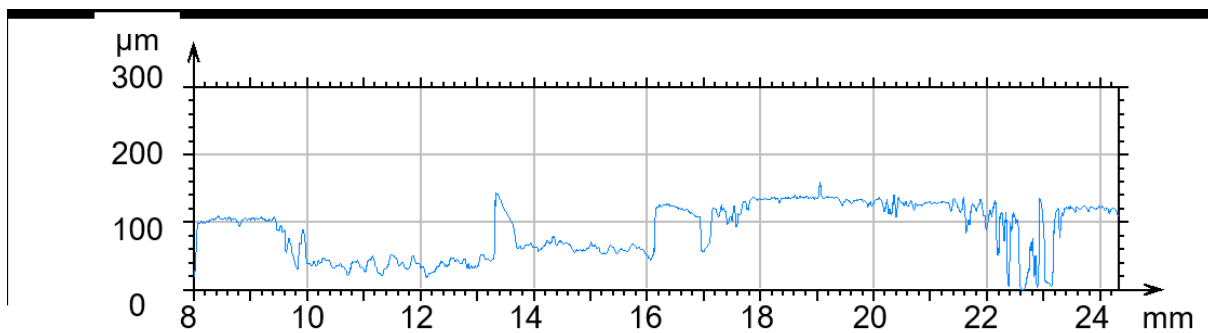


Figure 13. Surface roughness profile in the radial direction at an angle of 65° for the first characteristic zone on the disc surface

Figure 14 (a) illustrates the 3D surface topography, which occurs after a rotation between approximately 180° and 225°, where the maximum friction coefficient is reached (Figure 14 (b)). In this area, the accumulated oxides achieve a height of approximately 200 μm. Figure 14 (b) also illustrates that a decrease in the friction coefficient along the track is commonly associated with an increase in the operating speed, as indicated by the points labeled as (2) and (4). Also, the surface roughness profiles along this path are shown in Figure 14 (c) at the edge (I), middle (II) and close to the disc center (III) in the zone with accumulated oxides. The surface roughness profile in Figure 14 (c-I) exhibits the best correspondence with the friction coefficient curve shown in Figure 14 (b). Thus, the friction coefficient valley labeled as (2) in Figure 14 (b) matches the surface roughness valley, whereas the friction coefficient peaks (1) and (3) agree with the surface roughness plateaus. However, the valley (4) does not appear on the surface roughness profile. Nevertheless, the friction coefficient and surface roughness follow the same increasing trend.

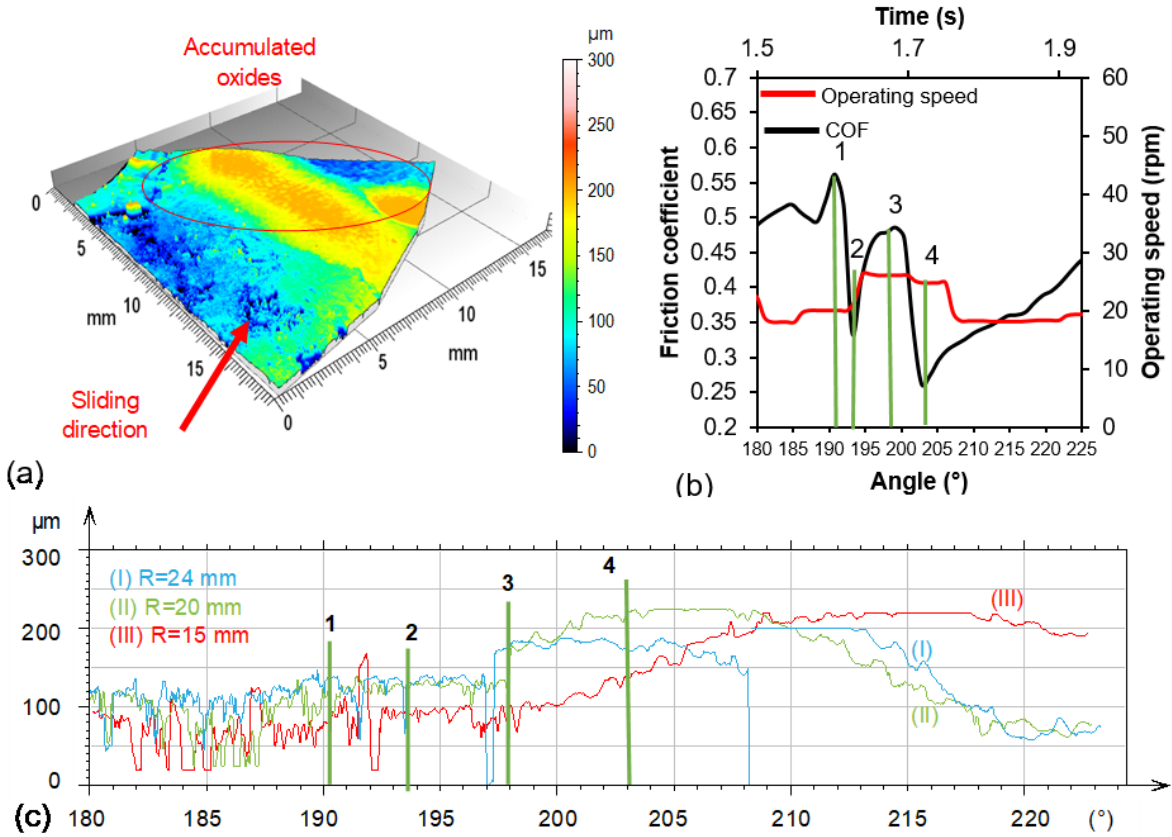


Figure 14. Second characteristic zone on the disc surface for Test Condition n°1: (a) 3D surface topography; (b) COF and operating speed curves; (c) surface roughness profiles at the edge (I), middle (II) and center (III);

Accordingly, the stick-slip mechanism at micro-scale can be divided into the following stages:

(I) The crushed oxides accumulate at the tool/billet contact zone, in front of the indenter and thus, the steel/oxide or lubricant/oxide contact conditions are transformed into an oxide/oxide contact condition. Under these circumstances the friction coefficient increases and the tool tends to stick to the sliding surface.

(II) In order to maintain the required operating speed, the machine accelerates and the velocity jumps, giving rise to the tool slip. The accumulated oxides leave the contact zone and the contact conditions partially transform again from an oxide/oxide to a steel/oxide condition, which brings about a decrease in the friction coefficient.

The above proposed mechanism is consistent with some results reported in the literature. Tieu et al. [20] reported that an iron oxide layer formed at 850°C was broken, peeled off and stuck onto the roll surface during the hot rolling tests. Similarly, Tran et al. [10] indicated in their study that the formed oxide scale layer sticks during pin-on-disc tests on a SS316 steel grade at 920°C.

3.3.2 Sensitivity to the contact parameters

Concerning the effect of the contact parameters on the stick-slip phenomenon, Figure 15 (a) illustrates the friction coefficient and the angular speed evolution curves for a roll-on-disc test in condition n°5. This mean coefficient was determined from the method proposed by Zambrano et al. [19] where the end of the running-in period is determined in terms of the intersection point resulting from drawing the slopes in the stable zone and the transition zone of the friction versus the angle curve. The friction coefficients in the rest of the document are determined in the same way.

The contact parameters are an interface temperature of 700°C, a mean operating speed of 4.8 rpm (sliding velocities from 4 to 12 mm/s) and a mean pressure of 200 MPa. A mean friction coefficient of 0.36 can be calculated along the sliding track, which corresponds to the lubricated conditions. On the other hand, Figure 15 (b) shows the friction coefficient and

velocity evolution curves at the same temperature and mean pressure, but for a rotating speed of 47.7 rpm (sliding velocities from 40 to 125 mm/s). The above results clearly indicate that under these testing conditions, the lubricant effect is negligible and therefore, the friction coefficient rapidly increases to a value of approximately 0.5-0.6. A maximum friction coefficient value of 0.6 has also been reported by Matsumoto et al. [8] during the hot forging ring compression tests on JIS SCr 420 steel oxidized samples at 1000°C.

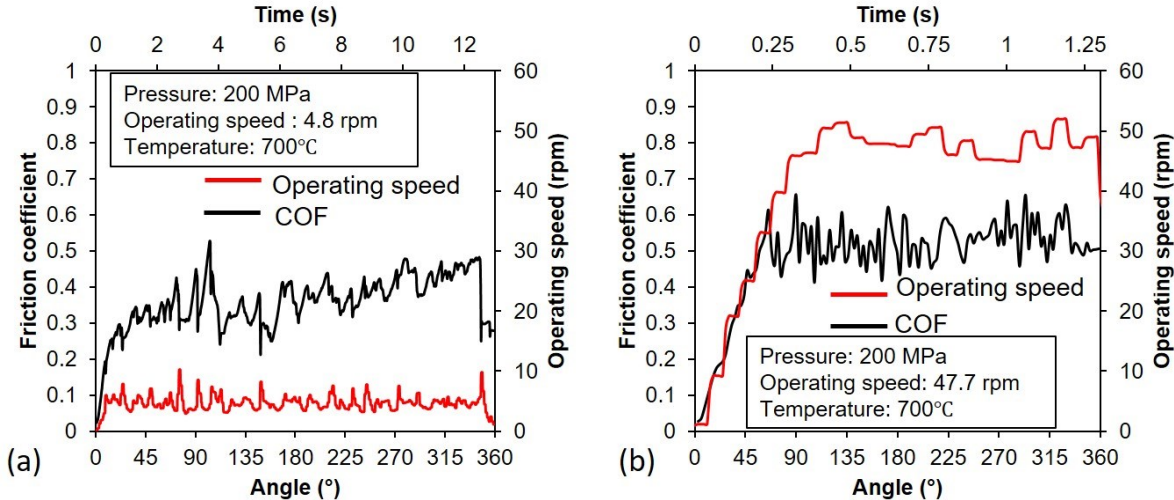


Figure 15. Change in the friction coefficient and operating speed evolution curves as a function of the angular rotation for two lubricated roll-on-disc tests conducted at the same temperature (700°C) and mean pressure (200 MPa), for different angular speeds: (a) 4.8 rpm (“slow” test, test conditions No. 5) and (b) 47.7 rpm (“fast” test, test conditions No. 6).

In order to analyze the stick-slip phenomenon at the operating speed of 4.8 rpm, the zone between 45° and 105° is chosen, as shown in Figure 16 (a). This area corresponds to the maximum friction coefficient value of 0.53 observed in Figure 16 (b). The peak of the accumulated oxides can be seen at the disc center on the 3D surface topography (Figure 16 (a)). The surface roughness profiles along the sliding distance are presented in Figure 16 (c). The friction coefficient and the speed evolution curves, as well as the analyzed surface roughness profile in Figure 16 (c-III) follow a similar change as that observed during the standard tests. The peaks of the accumulated oxides labeled as 1, 3 and 5 (Figure 16 (c-III)) correspond to the friction coefficient peaks and operating speed valleys. The oxide valleys (2) and (4) correspond to the speed peaks and friction coefficient valleys. At low speed (Figure 16 (b)), the oxide accumulation slows down the tool, the operating speed decreases and the coefficient of friction increases. The oxide is crushed and the tool slides again: the coefficient of friction with the

lubricant present returns to a value close to 0.3. The operating speed gradually returns to the specified value. The lack of correspondence of the surface roughness profiles in Figure 16 (c-I) and (c-II) and the friction coefficient curves is due to the small quantity of the accumulated oxides.

Here the stick stage is more visible in comparison with that observed at the rotating speed of 21 rpm, shown in Figures 12 and 14. This could be explained by less oxide accumulation rate under these conditions.

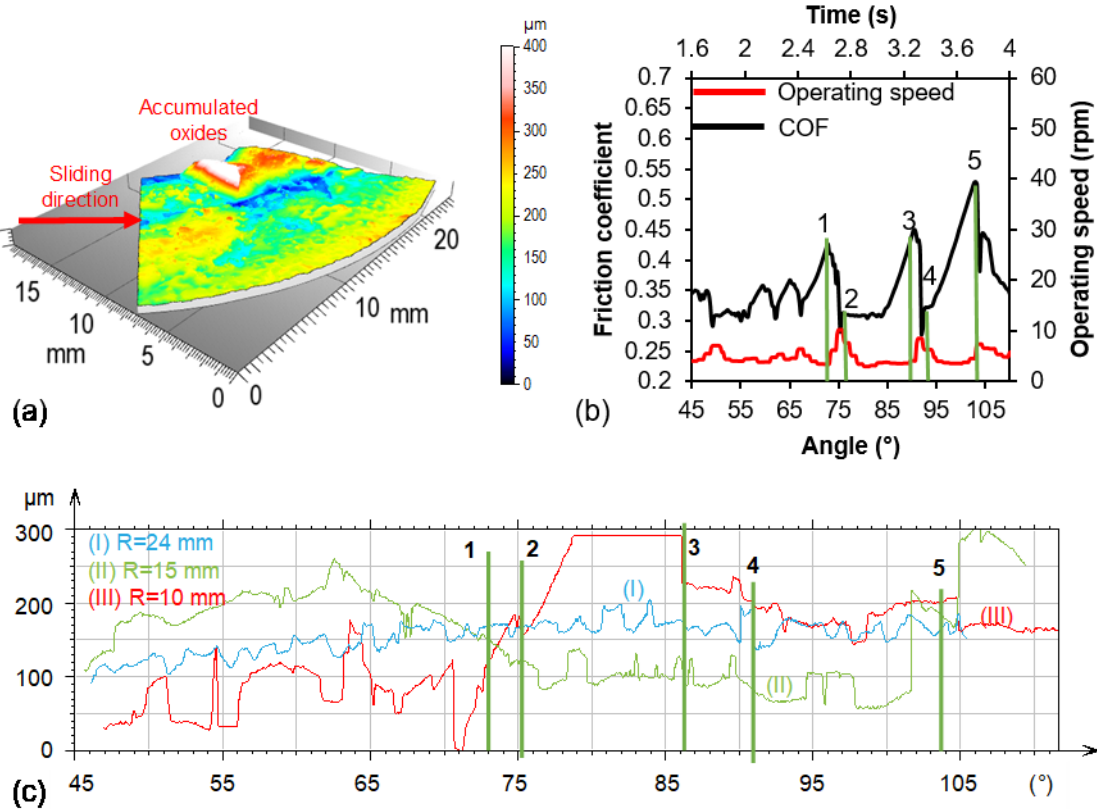


Figure 16. Characteristic zone on the disc surface for the “slow” roll-on-disc test: (a) 3D surface topography; (b) COF and operating speed curves; (c) surface roughness profiles at the edge (I), middle (II) and center (III);

Additionally, the stick-slip phenomenon is also analyzed for the “fast” roll-on-disc tests in Figure 15 (b). In this case, the friction coefficient curve exhibits a number of parasite oscillations, that is to say, a large number of oscillations, which do not correspond to the operating speed oscillation and that could be caused by machine vibration. Figure 17 presents the analysis of the characteristic zone between 200° and 244° on the disc surface. The accumulated oxide peak can be observed on the disc surface topography, as shown in Figure 17 (a). Similarly, a single friction coefficient peak in the analyzed area can be observed on the

friction evolution curve in Figure 17 (b). Figure 17 (c) illustrates the change in the surface roughness profiles along the sliding distance at the disc edge (I), middle (II) and center (III), corresponding to the zone with the accumulated oxides and at disc center, respectively. The accumulated oxide peak labeled as 1 in Figure 17 (c-II) corresponds to the friction coefficient peak and the speed valley shown in Figure 17 (b). However, the surface roughness peak 1 is observed to be sharper than its corresponding friction coefficient peak. Due to the effect of speed, the oxide is crushed faster and flows more easily.

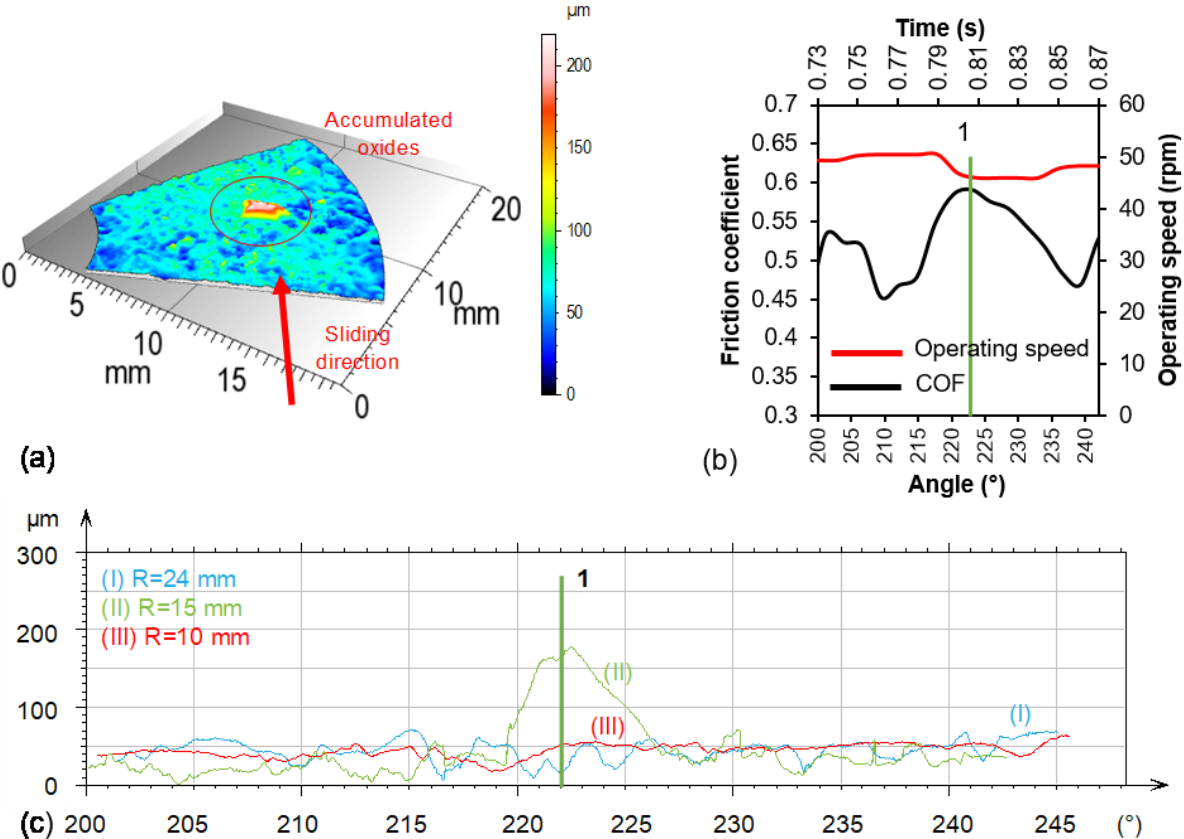


Figure 17. Characteristic zone on the disc surface for the “fast” roll-on-disc test: (a) 3D surface topography; (b) COF and operating speed curves; (c) Surface roughness profiles at the edge (I), middle (II) and center (III);

The surface roughness parameters are also analyzed along the sliding distance for different radii. Figure 18 illustrates the change in the root mean square of the local profile slope (R_{dq}) as a function of radial position, from the center to the edge of the disc. This parameter can be used to estimate the roughness at micro-scale [21]. These roll-on-disc tests are conducted at a pressure 200 MPa, a temperature 700°C and operating speeds 4.8 and 47.7 rpm, respectively.

The R_{dq} parameter is a hybrid parameter, which combines height and spacing surface information (Equation 2). It is measured in degrees and is defined as:

$$R_{dq} = \sqrt{\frac{1}{L} \int_0^L \left(\frac{dZ(x)}{dx} \right)^2 dx} \quad (2)$$

where L is the profile length and $\frac{dZ(x)}{dx}$ is the local roughness slope.

At an operating speed of 4.8 rpm, R_{dq} increases from center to edge, from approximately 1° to 4° . The maximum value is observed at a radius of 18 mm. Subsequently, R_{dq} slightly decreases from 4° to 3° at the edge.

The smoothest surface corresponds to the roll-on-disc tests, which were conducted at the highest operating speed of 47.7 rpm. This result can be explained by the removal of the accumulated oxides, which would confirm the lack of correlation between the peaks observed in Figure 16. Also, it can be assumed that the number of the stuck accumulated oxides increases with an increase in R_{dq} , as can be seen in Figures 15.

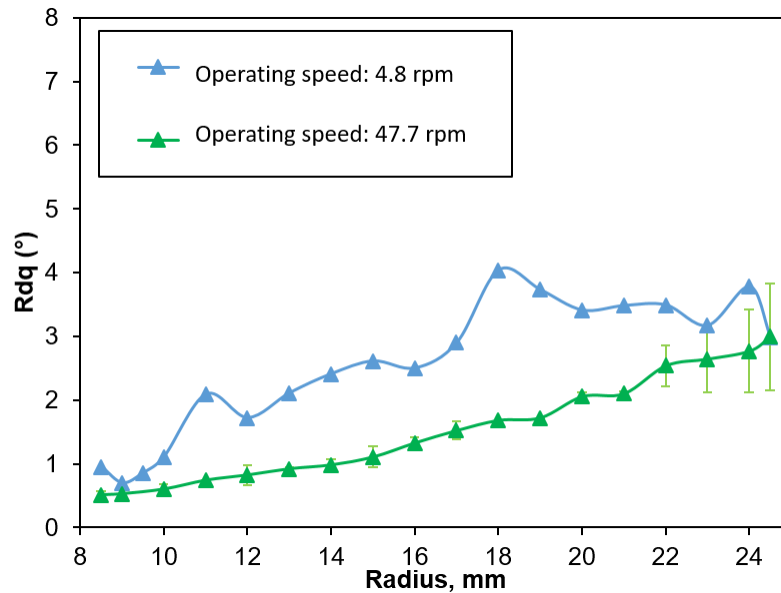


Figure 18. R_{dq} evolution from the center to the edge of the disc for the lubricated roll-on-disc tests conducted at a temperature of 700°C , a pressure of 200 MPa and two different angular speeds: 4.8 rpm and 47.7 rpm

Figures 19 (a) and (b) illustrate the friction coefficient and sliding angular speed evolution curves for the roll-on-disc tests conducted at 100 MPa and 250 MPa respectively. Under a contact pressure of 100 MPa, the lubricant effect can be observed at the beginning of the test (Figure 19 (a)): the friction coefficient is around 0.36, the stick-slip phenomenon occurs and the oxide accumulates at the contact. At an angle of approximately 80°, the lubricant film breaks down. Subsequently, the friction coefficient increases to the value corresponding to a non-lubricated specimen. Additionally, the friction coefficient decreases to the value corresponding to a lubricated condition after a rotation of 250°, which could be explained by the excess of lubricant stuck on the tool under the accumulated oxides at lower pressures. The friction coefficient oscillations are not consistent with the operating speed oscillations along the sliding curves. The operating speed exhibits a relatively stable behavior under the prescribed testing conditions, whereas the friction coefficient fluctuates significantly.

On the contrary on Figure 19 (b), the lubricant effect is negligible at a pressure of 250 MPa and the friction coefficient rapidly increases to the value characteristic of the non-lubricated sample. Additionally, as the contact pressure increases, a regular stick-slip behavior occurs. Thus, the friction coefficient and operating speed oscillations are consistent along the sliding distance.

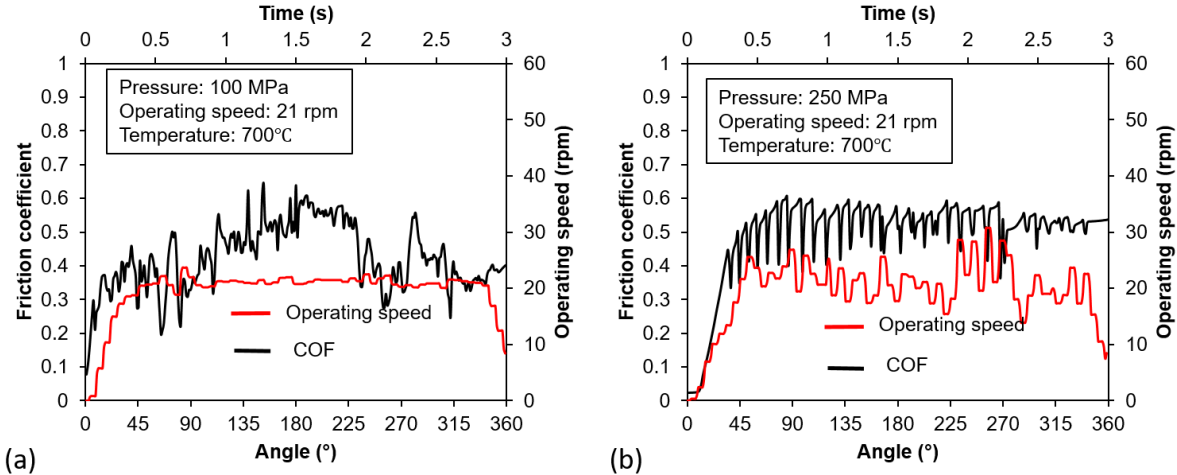


Figure 19. Friction coefficient and operating speed evolution during the lubricated roll-on-disc tests with variable pressure at a temperature of 700°C and an operating speed of 21 rpm: (a) 100 MPa (Test conditions No. 3) (b) 250 MPa (Test conditions No. 4)

As noted in the previous sections, the interface contact temperature can increase up to 800°C during the hot forging contact. The Figure 20 illustrates the results for a roll-on-disc test conducted at a pressure of 200 MPa, an operating speed of 21 rpm and a temperature of 800°C. The friction coefficient increases up to the non-lubricated conditions value after a rotation of 30°, before the indenter achieves the required operating speed of 21 rpm. It can be assumed that at 800°C, the soap lubricant layer loses its lubrication properties and therefore, the contact conditions correspond to the non-lubricated ones. Then an investigation on the lubricant layer breakdown mechanism has been performed.

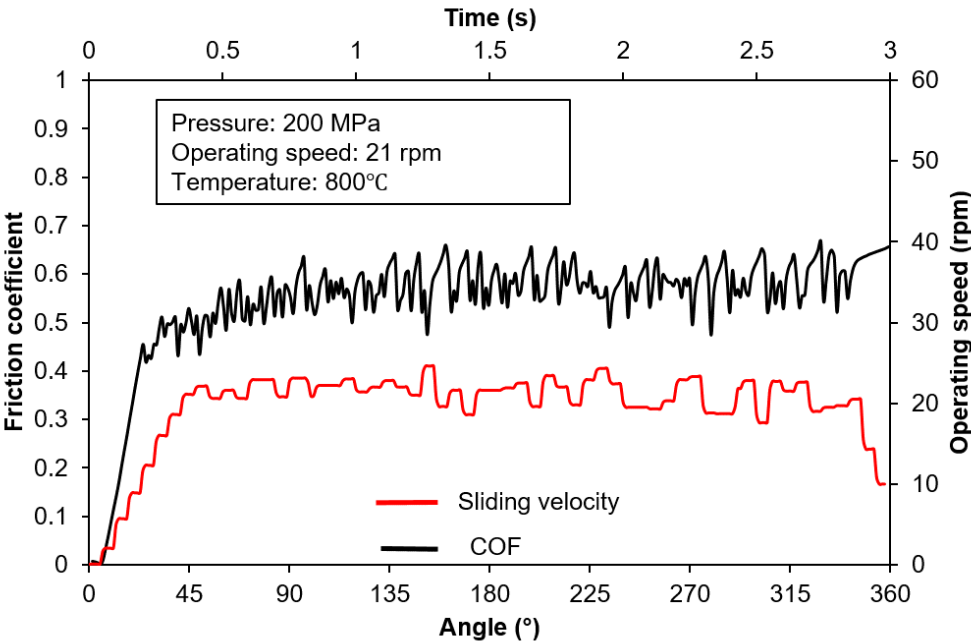


Figure 20. Friction coefficient evolution during the lubricated roll-on-disc tests conducted at a pressure of 200 MPa, an operating speed of 21 rpm and a temperature of 800°C (Test conditions No. 2)

3.3.3 Lubricant film breakdown mechanism

Figures 21 (a) and (b) illustrate the friction coefficient evolution curves along the sliding track for the non-lubricated and lubricated conditions during the roll-on-disc tests conducted at a temperature of 700°C, an operating speed of 21 rpm and a mean pressure of 200 MPa. The analysis of such curves indicates that the 20% soap-water lubricant clearly influences the friction coefficient under the applied contact conditions at micro-scale. Under the non-lubricated conditions, the friction coefficient is characterized by a rapid increase from 0, at the

beginning of the test, to approximately 0.67 following a rotation of approximately 45°, after which the COF stabilizes at a value of about 0.5.

When the tests are conducted under lubricated conditions, the friction coefficient rapidly increases from 0 to 0.3 after a rotation to an angle of approximately 22°. Subsequently, the COF continues to increase at a smaller rate until it stabilizes at a value of about 0.5 following a rotation of approximately 90°. This stage corresponds to the lubricant film breakdown, as indicated in Figure 21 (b). After the removal of the lubricant film, the COF evolution is similar to that observed during the stabilized period of the non-lubricated tests.

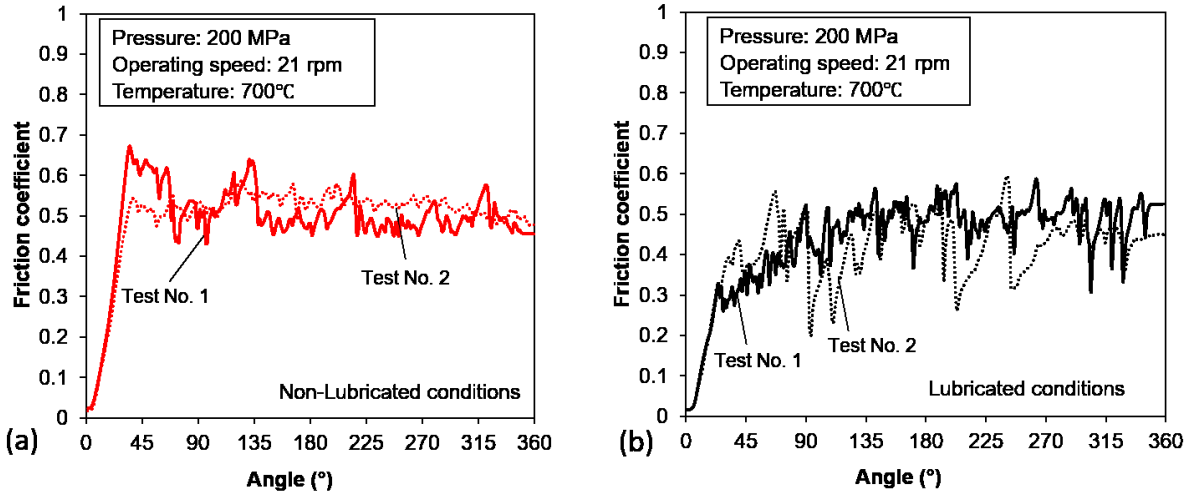


Figure 21. Friction coefficient evolution during the roll-on-disc tests: (a) non-lubricated conditions (Test condition No. 7), (b) lubricated conditions (Test condition No. 1)

In order to investigate in more detail the lubricant transfer mechanism from the tool to the disc, SEM-EDS analyses are carried out on both surfaces after roll-on-disc tests at a temperature of 700 °C using a contact pressure of 200 MPa and a rotating speed of 21 rpm (Test conditions No. 1). Table 3 reports the chemical elements of interest (%wt) obtained by EDS analyses of the areas shown in Figures 22-24.

Table 3. Chemical elements (%wt) obtained by EDS analyses.

Figure	Chemical element (%wt)		
	Fe	O	Na
22(a)	53.5	39.6	6.9
23(a)	80.6	19.3	0.1
24(a)	71.7	26.3	2.0

24(e)	69.6	28.9	1.5
-------	------	------	-----

Figure 22 corresponds to a non-contact edge of the originally lubricated tool where different contrast regions can be observed (Figure 22 (a)). As expected, the base metal (Figure 22(b)) is mostly covered by the lubricant layer, which contains Na as one of its main elements (Figure 22 (d)). In contrast, when the contact edge of the tool is analyzed, its worn surface is clearly exposed (Figure 23(a) and (b)), whereas the lubricant layer has been depleted remaining only a few traces of Na (Figure 23 (d)).

Regarding the study carried out on the disc, traces of the lubricant are found mainly in the first millimeters of the wear track on the cracked oxide layers still adhered to the disc (Figure 24). Wang et al. [2] have also reported that lubricant elements traces could be found on the oxidized disc surface after a ball-on-disc test at 920 °C. Thus the transfer of the lubricant layer from the tool to the disc contributes to the sliding between surfaces, leading to a reduction of the friction coefficient in this tribosystem, as compared to the non-lubricated one.

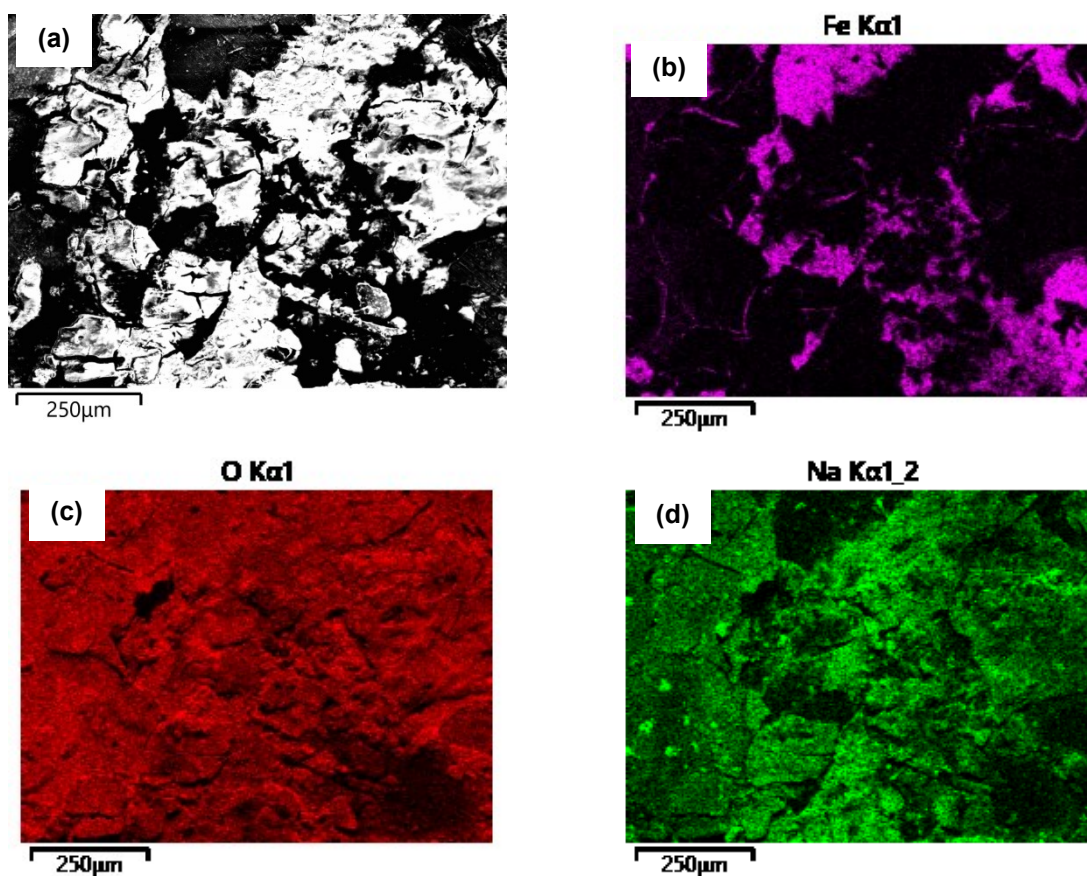


Figure 22. Non-contact edge on the tool showing the presence of a lubricant layer after the roll-on-disc test (Test conditions No. 1). (a) and (d) secondary electron image. (b), (c) and (d) EDS elemental mapping of Fe, O and Na, respectively.

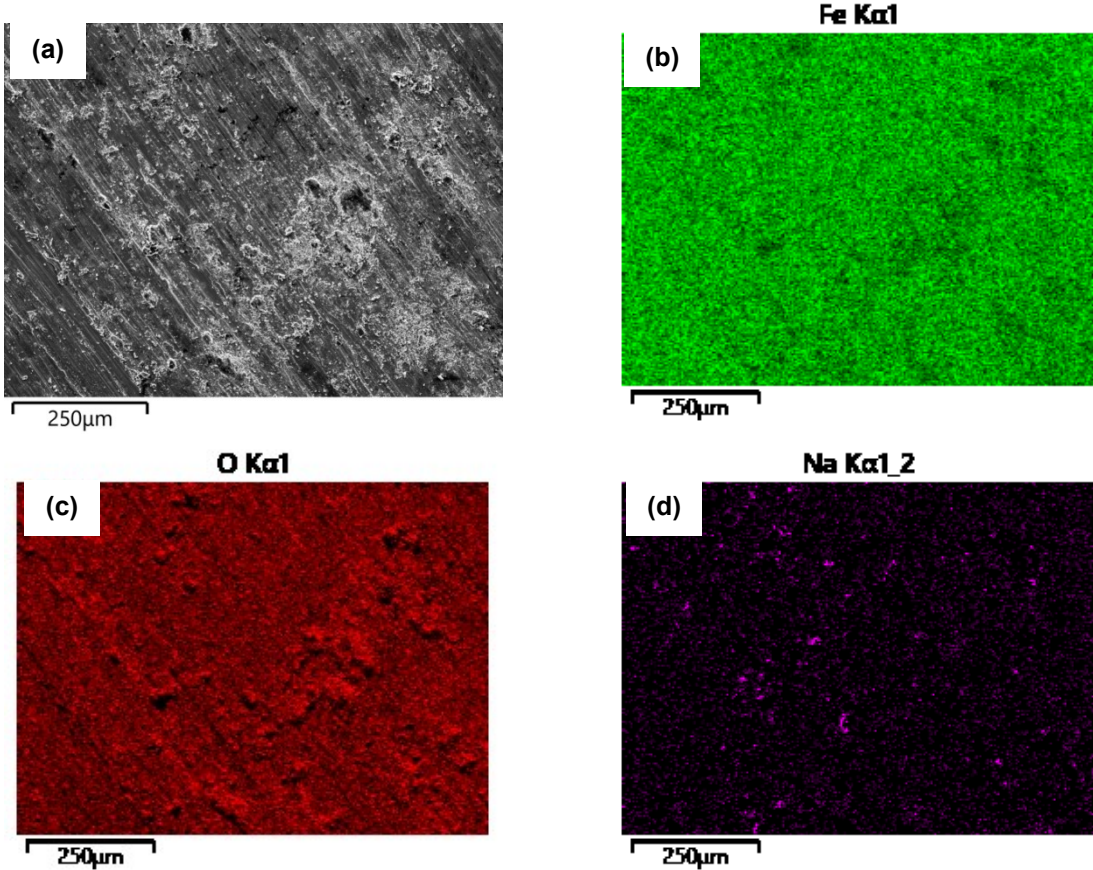
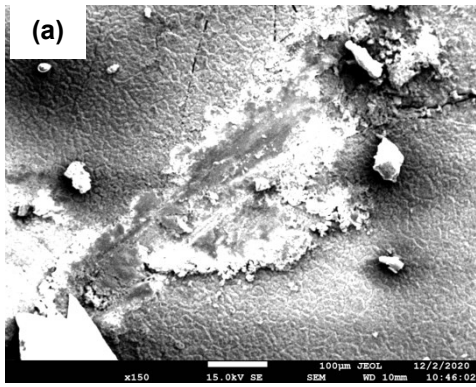
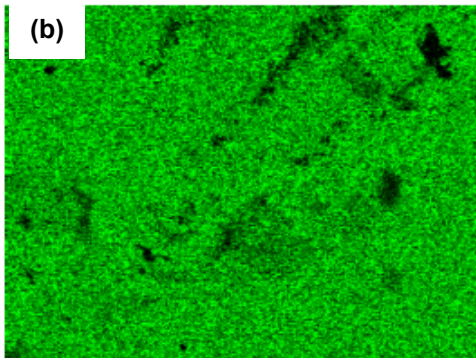


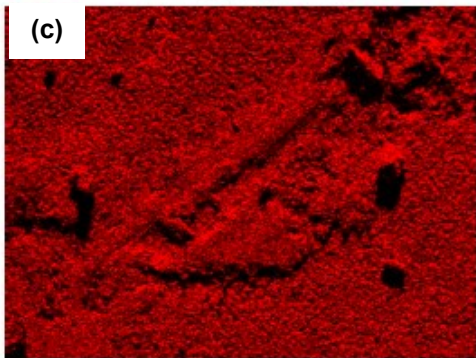
Figure 23. Contact edge on tool surface showing depletion of lubricant layer after the roll-on-disc test (Test conditions No. 1). (a) secondary electron image. (b), (c) and (d) EDS elemental mapping of Fe, O and Na, respectively.



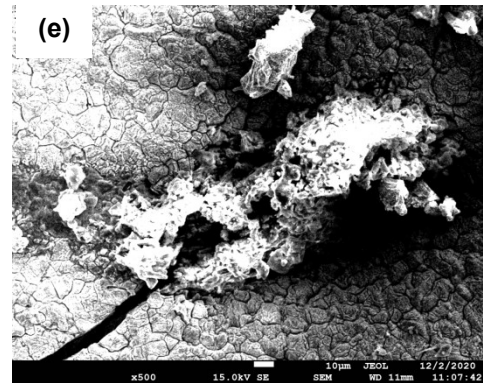
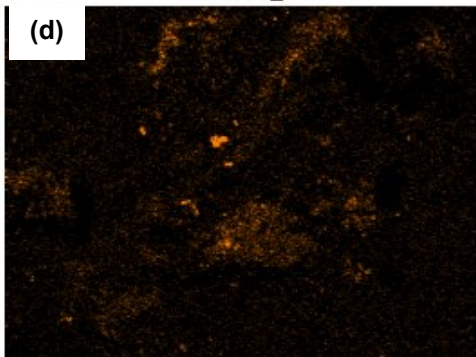
Fe Kα1



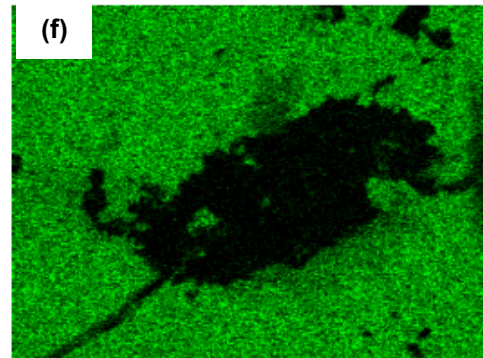
O Kα1



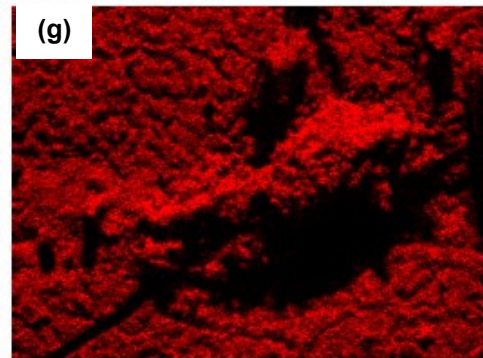
Na Kα1_2



Fe Kα1



O Kα1



Na Kα1_2

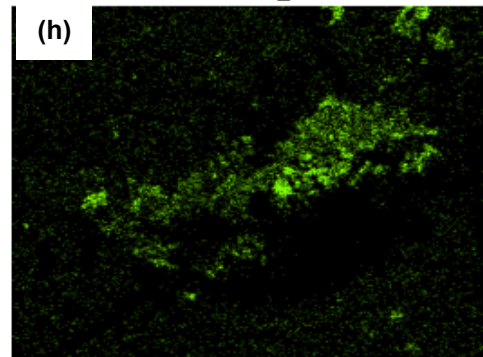


Figure 24. Worn disc surface (Test conditions No. 1). (a) and (e) secondary electron images obtained at the beginning of the wear track. (b) and (f), (c) and (g), (d) and (h) EDS elemental mapping of Fe, O and Na, respectively.

4 Conclusions

A multiscale methodology has been applied to analyze the friction phenomena during the hot forging of railway wheels. This leads to the following conclusions:

At the macro-scale, the interface conditions are obtained from an analysis of the industrial forging process and from FEM simulations. According to the operating parameters (contact pressure, contact temperature, sliding velocity) and the interface constituents (lubricant, oxide layer), a reduced-scale analysis has been designed to reproduce locally these conditions.

At the meso-scale, the observations of the specimens show that the friction evolution of a lubricated sliding test can be described in two stages: a lubricant/oxide interface defines the friction conditions in a first step, then an oxide/oxide interface leads to different friction conditions. The observations can be correlated with the friction coefficient value. In the first step, the friction coefficient is in the range of 0.2-0.4, then it increases to 0.4-0.8 in the oxide/oxide interface for the WHUSTs. Moreover, the analysis of the specimen's cross section after hot upsetting-sliding tests indicates that the initial tri-layer oxide structure formed during the preheating time is transformed into a bi-layer film constituted mainly by crushed and embedded oxides. The influence of the oxide layer and of the lubricant film breakdown has been investigated with the roll-on-disc test.

At the micro-scale, it was found that the friction coefficients are similar to the values found at the meso-scale tests. The friction coefficient was found to be in the range of 0.2-0.4 at the lubricant/oxide stage, whereas at the oxide/oxide contact stage, the friction coefficient changed in the range of 0.4-0.7. As compared to the WHUST, this micro-scale approach allows a highlight of the stick-slip phenomena which occurs with the accumulation / breakage of the thin oxide layer ahead of the tool. The optical topography demonstrates a link between oxides peak / valleys and the variation of the friction coefficient and the sliding velocity.

Additionally, the friction and operating speed evolution curves obtained from the roll-on-disc tests indicates that the lubricant film breaks down prior to tool sticking due to the

accumulation of the crushed oxides ahead of the tool. The EDS analyses of tools and tested specimens also indicate that the soap lubricant is entirely transferred to the sample surface during the sliding at micro-scale.

It has been determined that at testing temperatures in the range of 700°C to 800°C and contact pressures in the span 200 to 250 MPa, the lubricant effect is negligible when the tests are carried out at elevated angular velocities (47.7 rpm), that is to say, above linear velocities in the range of 40-125 mm/s.

Acknowledgments

The authors gratefully acknowledge the financial support of Valenciennes Metropole granted to I. Serebriakov and to Professor Puchi-Cabrera, as well as the infrastructure provided by the Science for Wheelset Innovative Technology laboratory (SWIT'lab), Université Polytechnique Hauts de France, Valenciennes, France. The special collaboration of S. Salengro and F. Demilly (MG Valdunes) is also gratefully acknowledged.

References

- [1] Yu X, Jiang Z, Zhao J, Wei D, Zhou J, Zhou C, et al. The role of oxide-scale microtexture on tribological behaviour in the nanoparticle lubrication of hot rolling. *Tribology International* 2016;93:190–201. <https://doi.org/10.1016/j.triboint.2015.08.049>.
- [2] Wang L, Tieu AK, Cui S, Deng G, Wang P, Zhu H, et al. Lubrication mechanism of sodium metasilicate at elevated temperatures through tribo-interface observation. *Tribology International* 2020;142:105972. <https://doi.org/10.1016/j.triboint.2019.105972>.
- [3] Behrens B-A, Chugreev A, Awiszus B, Graf M, Kawalla R, Ullmann M, et al. Sensitivity Analysis of Oxide Scale Influence on General Carbon Steels during Hot Forging. *Metals* 2018;8:140. <https://doi.org/10.3390/met8020140>.
- [4] Zambrano OA, Gallardo KF, Polania DM, Rodríguez SA, Coronado JJ. The Role of the Counterbody's Oxide on the Wear Behavior of HSS and Hi-Cr. *Tribology Letters* 2018;66. <https://doi.org/10.1007/s11249-017-0954-1>.
- [5] Cui S, Zhu H, Wan S, Tran B, Wang L, Tieu K. Investigation of different inorganic chemical compounds as hot metal forming lubricant by pin-on-disc and hot rolling. *Tribology International* 2018;125:110–20. <https://doi.org/10.1016/j.triboint.2018.04.010>.
- [6] Utsunomiya H, Nakagawa T, Matsumoto R. Mechanism of oxide scale to decrease friction in hot steel rolling. *Procedia Manufacturing* 2018;15:46–51. <https://doi.org/10.1016/j.promfg.2018.07.168>.

- [7] Cheng X, Jiang Z, Wei D, Hao L, Zhao J, Jiang L. Oxide scale characterization of ferritic stainless steel and its deformation and friction in hot rolling. *Tribology International* 2015;84:61–70. <https://doi.org/10.1016/j.triboint.2014.11.026>.
- [8] Matsumoto R, Osumi Y, Utsunomiya H. Reduction of friction of steel covered with oxide scale in hot forging. *Journal of Materials Processing Technology* 2014;214:651–9. <https://doi.org/10.1016/j.jmatprotec.2013.10.011>.
- [9] Behrens B-A, Kawalla R, Awiszus B, Bouguecha A, Ullmann M, Graf M, et al. Numerical Investigation of the Oxide Scale Deformation Behaviour with Consideration of Carbon Content during Hot Forging. *Procedia Engineering* 2017;207:526–31. <https://doi.org/10.1016/j.proeng.2017.10.816>.
- [10] Tran BH, Tieu K, Wan S, Zhu H. Lubricant as a sticking-scale inhibitor on high temperature sliding contact. *Tribology International* 2019;140:105860. <https://doi.org/10.1016/j.triboint.2019.105860>.
- [11] Kong N, Tieu AK, Zhu Q, Zhu H, Wan S, Kong C. Tribofilms generated from bulk polyphosphate glasses at elevated temperatures. *Wear* 2015;330–331:230–8. <https://doi.org/10.1016/j.wear.2015.02.042>.
- [12] Bao Y, Sun J, Kong L. Effects of nano-SiO₂ as water-based lubricant additive on surface qualities of strips after hot rolling. *Tribology International* 2017;114:257–63. <https://doi.org/10.1016/j.triboint.2017.04.026>.
- [13] Dubois A, Dubar M, Dubar L. Warm and Hot Upsetting Sliding Test: Tribology of Metal Processes at High Temperature. *Procedia Engineering* 2014;81:1964–9. <https://doi.org/10.1016/j.proeng.2014.10.265>.
- [14] European Standard EN 13262, 2020, “Railway Applications – Wheelsets and Bogies – Wheels – Product Requirement” n.d.
- [15] Dubar L, Dubois A, Dubar M. Friction and Wear in Metal Forming: 25 Years at LAMIH UMR CNRS 8201. *Key Engineering Materials* 2018;767:42–58. <https://doi.org/10.4028/www.scientific.net/KEM.767.42>.
- [16] Lazzarotto L, Dubar L, Dubois A, Ravassard P, Oudin J. Identification of Coulomb’s friction coefficient in real contact conditions applied to a wire drawing process. *Wear* 1997;211:54–63. [https://doi.org/10.1016/S0043-1648\(97\)00080-X](https://doi.org/10.1016/S0043-1648(97)00080-X).
- [17] Daouben E, Dubois A, Dubar M, Dubar L, Deltombe R, Truong Dinh NG, et al. Effects of lubricant and lubrication parameters on friction during hot steel forging. *International Journal of Material Forming* 2008;1:1223–6. <https://doi.org/10.1007/s12289-008-0162-5>.
- [18] Puchi-Cabrera ES, Guérin J-D, La Barbera-Sosa JG, Dubar M, Dubar L. Effect of initial grain size on the mechanical behaviour of austenite during deformation under hot-working conditions. *Materials Science and Engineering: A* 2020:139553. <https://doi.org/10.1016/j.msea.2020.139553>.

- [19] Zambrano OA, Coronado JJ, Rodríguez SA. Tempering Temperature Effect on Sliding Wear at High Temperatures in Mottled Cast Iron. *Tribology Letters* 2015; 57(2): 19. doi: 10.1007/s11249-014-0462-5
- [20] Tieu AK, Zhu Q, Zhu H, Lu C. An investigation into the tribological behaviour of a work roll material at high temperature. *Wear* 2011;273:43–8. <https://doi.org/10.1016/j.wear.2011.06.003>.
- [21] Cabanettes F, Joubert A, Chardon G, Dumas V, Rech J, Grosjean C, et al. Topography of as built surfaces generated in metal additive manufacturing: A multi scale analysis from form to roughness. *Precision Engineering* 2018;52:249–65. <https://doi.org/10.1016/j.precisioneng.2018.01.002>.